

Review Article

Plasmonic Nanoparticles and Their Conjugates: Preparation, Optical Properties and Antimicrobial Activity

Ignac Capek

Slovak Academy of Sciences, Polymer Institute, Institute of Measurement Science, Bratislava, Slovakia and Faculty of Industrial Technologies, TnUni, Púchov, Slovakia

Received date: February 1, 2015

Accepted date: April 16, 2015

Published date: April 22, 2015

Citation: Capek, I. Plasmonic Nanoparticles and their Conjugates: Preparation, Optical Properties and Antimicrobial Activity. (2015) *J Nanotech Mater Sci* 2(1): 14- 31.

***Corresponding author:** Capek, I. Slovak Academy of Sciences, Polymer Institute, Institute of Measurement Science, Bratislava, Slovakia and Faculty of Industrial Technologies, TnUni, Púchov, Slovakia. E-mail: Ignac.Capek@savba.sk

Keywords: Noble metal nanoparticles; preparation; properties; surface Plasmon; bio conjugates

Abstract

To manipulate the size of noble metal particles on a nanometer scale are priority subjects in the field of nanotechnology. So far various approaches have been developed to synthesize noble metal nanoparticles in controlled sizes and dimensions. Among them the colloidal systems become broadly used. These systems can be made up of several very different reactants and solvents: a continuous medium water or alkane, surfactant and precursor(s). In some systems the formation of (sub) nanoparticles is based on the supersaturation of solution by reactants. The existence of the microenvironments gives them a particular ability to modulate the chemical reactivity of the reactants due to their compartmentalization in different microenvironments. The size and shape of noble metal nanoparticles follow the feed composition of reactants in the precursor solution, the reaction conditions and concentration and type of reactants. Surface modification and functionalization is expected to increase the stability of nanoparticles and organize them to the assembly of higher order array conjugates. Various soft and hard templates can be applied to produce noble metal nanoparticles in different shaped nanoreactors. Monodisperse gold nano crystals can grow inside soft templates and the cavities of hard templates by the reduction of metal ions trapped in the cavities. The interesting optical properties of noble metal nanoparticles and their (bio)conjugates results from the strong absorption in the visible spectrum region, so called the surface plasmon absorption. Some noble metal nanoparticles have been studied for their antimicrobial potential and have proven to be antibacterial and antiviral agents.

Introduction

The gold nanoparticles have fascinated researchers since historic times because of their unique colors, size and shape dependent optical properties and environmental stability. While the most ancient use of colloidal gold is believed to have been in China and Egypt by alchemists, the brilliant colors of nanosized colloidal particles of silver, gold and copper were used in staining glasses as back as the 17th century. The use of gold colloid in biological applications began in our centuries, when the immunogold staining procedure, surface particle modifications and bio decoration of noble metal nanoparticles were invented.

The preparation of (noble) metal nanoparticles has received considerable attention in recent decades because nanoparticles possess unconventional physical and chemical properties^[1]. The unique physical properties of metal nanoparticles or fluid have generated considerable interest for their use in a wide range of diverse applications from templates for different probes to in vivo optical and magnetic manipulation in biomedical systems^[2]. In particular, due to their large surface-to-volume ratio, the optical and magnetic properties of nanoparticles are dominated by surface effects, particle-particle and particle-sup-

port interactions and surface particle reactivity^[3]. Nanoparticles exhibit novel material properties which largely differ from the bulk materials due to these small sizes, including quantum size effect on photochemistry, nonlinear optical properties of semiconductor or the emergence of metallic properties with the size of the particles, the high penetration efficiency into the cells and energy storing ability. Zero-(0D) and one-dimensional (1D) noble metal nanoparticles have extensive applications, such as antibacterial materials^[4], two-dimensional (2D) and three-dimensional (3D) assemblies can act as antistatic materials, cryogenic superconducting materials^[5] and biosensor materials.

Many nanogold and nanosilver based environmental technologies (e.g., sensors, sorbents, reactants, templates, bio-probes,) are under very active research and development, and are expected to emerge as the next generation environmental technologies to improve or replace various conventional environmental technologies^[6]. Some of the most promising near term realizations of nanotechnology are at the interface of 0D, 1D or 2D particles and their conjugates and assemblies. Because many biomolecules have specific binding properties in self-assembly processes, the bio decorated nanoparticles and their self-assemblies are attractive materials for nanotechnology.

Organically functionalized or bio decorated metal

nanoparticles are prepared by several approaches. Most existing approaches explore the strong affinity of thiols to gold and silver^[7] and the use of disulfides^[8] and thioethers^[9] as capping and stabilizer agents as well. Polymers functionalized with molecular recognition groups^[10], thioacetate groups^[11], amino and carboxylate groups and tetradentate thioether ligands^[12] have recently been used to mediate the formation of colloidal stable 0D or 1D nanoparticles or related assemblies of two or three-dimensional gold and silver nanoparticles assemblies.

UV-visible spectroscopy is a valuable tool for the light absorbance and structural characterization of silver and gold nanoparticles as well. It is well known that the optical absorption spectra of noble metal nanoparticles are dominated by surface plasmon resonances (SPR), which is shifted to longer wavelengths with increasing particle size, increased particle aggregation, 1D particle formulation and 2D and 3D assemblies. We could also mention that the surface plasmon resonance of individual gold metal (especially gold and silver) nanoparticles make them ideal candidates for molecular labeling and fluorescence probe formulation, where phenomena such as surface enhance Raman scattering (SERS) can be exploited.

Silver and gold have long been known for its antimicrobial properties. Noble metal nanoparticles are reported to show antimicrobial, antibacterial and antiviral properties. Silver's mode of action is presumed to be dependent on Ag^+ ions, which strongly inhibit bacterial growth through suppression of respiratory enzymes and electron transport components and through interference with DNA functions^[13]. It is interesting to note that silver atoms and their aggregates (sub and nanoparticles) shows the similar activities as their cations. This was highlighted in medicine where the potential of metal nanoparticles has been explored for early detection, diagnosis, and treatment of diseases^[14].

Synthetic Approaches

Gold and Silver Nanoparticles

A number of techniques have been used for producing nanoparticles, including vapor phase techniques^[15], sol-gel methods^[16], sputtering^[17], coprecipitation^[18] etc. Two main methods can be employed for the preparation of noble metal nanoparticles: coprecipitation (supersaturation) and chemical reduction. In both cases, the presence of surfactant is required to govern the growth process and the particle agglomeration. Typically, the coprecipitation reactions involve the thermal decomposition of organometallic precursors^[19]. The chemical reduction occurring in colloidal assemblies is another approach for the formation of size and shape controlled nanoparticles^[20]. A major benefit of chemical methods is their relatively inexpensive investment of capital equipment.

Gold nanomaterials have also been synthesized using a variety of methods, including hard template, chemical and bioreduction and synthesis in micellar solutions (soft templates)^[21,22]. The successful utilization of silver or gold nanoparticles (AgNPs or AuNPs) in biological assays relies on the availability of synthetic methods generating nanoparticles with the desired characteristics, namely high solubility in both oil and water, and adequate morphology, size dispersion, and surface functionalities. Most commonly, gold nanoparticles are synthesized by chemical or electrochemical reduction of a gold (III) precursor compound in the presence of a capping agent, i.e. a compound able

to bind to the nanoparticle surface blocking its growth beyond the nanometer range and stabilizing the colloid in the particular solvent used. Control over the shape and size of the AuNPs is usually achieved through the careful selection of the experimental conditions, namely reducing agent, reaction time, temperature, and capping agent. A common approach is to use capping agents with strong affinity for gold, e.g. thiol capping agents. This allows the synthesis of AuNPs with good size dispersion but usually only soluble in organic solvents^[7] requiring an additional step of extraction of the particles into water. In addition, exchange of strongly binding capping agents is usually cumbersome, which makes this type of AuNP less versatile for biological applications. Due to its simplicity and high yield, the most commonly used method for preparation of spherical AuNPs for biological assays is the citrate reduction method^[23]. The use of citrate as a weak capping agent is very convenient due to its easy post-synthesis treatment, since it can be easily replaced by other capping agents, e.g. thiol capping agents, bearing an appropriate functionality for binding of the biological analyte of interest.

The co-precipitation (homogeneous and heterogeneous nucleation) of prime nanoparticles is based on the supersaturation of solution by reactants such as precursors (metal salts), reducing agent, stabilizers, co-stabilizers and additives. The increased solubility of component in the continuous phase can be reached by the rising in temperature. The supersaturation state can be then reached by the reduction in temperature. Generation of super saturation through in situ chemical reactions by converting highly soluble chemicals into less soluble chemicals is a good example of this approach. In a typical homogeneous nucleation synthesis consisting of one step process in which precursor(s), stabilizer(s) and other additives are stirred in the oil or water continuous phase and then treated by the heat^[24]. The heterogeneous nucleation of metal particles consists of several steps process^[2]. In a typical heterogeneous nucleation the first step is the formation of the primary (seed) metal particles (or using the solid surfaces) and then the growth of sub nanoparticles is achieved by the addition of precursor(s), stabilizer(s) and additives[Figure 1].

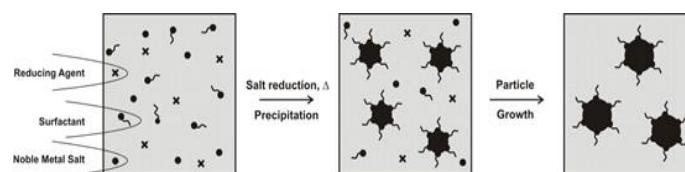


Figure 1. Proposed mechanism for the formation of noble metal nanoparticles by the supersaturation/precipitation approach^[24].

Whether these colloids are stabilized or undergo aggregation depends on the net potential of interparticle attraction and repulsion forces. The interparticle attraction force is van der Waals force, which is responsible for the nanoparticle aggregation. The two major repulsion forces that contribute to noble metal nanoparticle stabilization are electrostatic and steric repulsion forces^[25]. Electrostatic repulsion results from the negatively or positively charged ionic groups at ionic stabilizers. The charges, together with the counter ions in the medium, form a repulsive electric double layer that stabilizes colloids against van der Waals attraction^[26]. A characteristic feature of the electrostatic repulsion force is that it is highly sensitive to the bulk ionic strength: the electrostatic repulsion force diminishes sig-

nificantly at high salt concentration where electric double layer is highly suppressed. Steric stabilization (and/or polymeric stabilization)^[25] is another key contribution to the repulsion forces in the current system. Amphiphilic block copolymers and/or macromolecules grafted on colloid surfaces impart a polymeric barrier that prevents colloids from coming close enough such that van der Waals attractive forces can dominate. Steric stabilization is highly dependent on the thickness of polymer layer and surface graft density. In general, thicker polymer layers and higher graft densities lead to more effective steric stabilization effect.

Hiramatsu and Osterloh have used a high temperature solution phase synthesis as an inexpensive, versatile, and very reproducible method for the large-scale synthesis of organoamine protected gold and silver nanoparticles in the 6–21 nm (Au) and 8–32 nm (Ag) size ranges and with polydispersities as low as 7%^[27]. In terms of achievable particle sizes, polydispersities, and simplicity (only three reagents, tetrachloroauric acid, oleylamine, and a solvent are required) the method is superior to that of Jana et al.^[28]. The particles are stable in dried form and they can be easily modified with hydrophobic and hydrophilic thiols to afford nanoparticles that are soluble in organic solvents or in water. Organoamine protected gold and silver nanoparticles of variable sizes form by refluxing a solution of tetrachloroauric acid, silver acetate and oleylamine in toluene.

Of the chemical processes, reverse micelle (microemulsion) synthesis has been recently demonstrated to be a viable method for producing a wide array of metals and metal oxide nanoparticles^[29] over a relatively narrow particle size distribution. Reverse micelle synthesis utilizes the natural phenomenon involving the formation of spheroidal aggregates in a solution when a surfactant is introduced to an organic solvent, formed either in the presence or in the absence of water^[30]. Micelle formation allows for a unique encapsulated volume of controllable size through which reactions and subsequent development of metal and metallic compounds can be produced. Aggregates containing ω ($= [\text{water}]/[\text{surfactant}]$) of less than 15 can be called as reverse micelles and have hydrodynamic diameters in the range of 4–10 nm^[31], whereas ω greater than 15 constitute microemulsions, which have a hydrodynamic diameter range between 5 and 50 nm. Once the right microemulsions are obtained, the method of particle preparation consists in mixing of two microemulsions carrying the appropriate reactants in order to start the particle nucleation and obtain the desired nanoparticles^[32] [Figure 2].

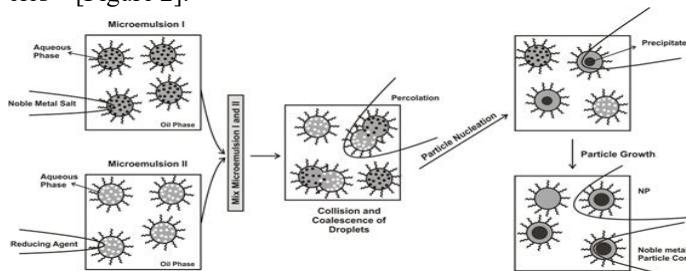


Figure 2. Proposed mechanism for the formation of metal particles by the microemulsion approach^[33].

Controlled nucleation and separation of nucleation from growth are the keys to synthesizing near monodisperse gold nanoparticles in the 1–15 nm size range^[33, 34]. This can be

achieved either by providing a controlled number of preformed gold nanoparticles as nucleation centers in a growth medium where no secondary nucleation can occur the seeding growth method^[34] or by varying the ratio of strong and weak reducing agents^[28]. Key goals in the synthesis of metal nanostructures are that the synthesis gives nanostructures of a specific size and size distribution and that the synthesis is reproducible^[35]. The simplest approaches for isotropic and anisotropic nanoparticle synthesis are various surfactant-based methods^[36]. Surfactant-based anisotropic micelle templates can be easily prepared^[37]. For example, the ~ 6 nm spherical micelles formed by a dilute (>1 mM) solution of cetyltrimethyl ammonium bromide surfactant converts to cylindrical micelles at higher concentrations (>20 mM), more elongated rod like micelles in the presence of organic solubilizers^[38], and worm like micelle structures in the presence of salicylate^[39]. Surfactant molecules can be used as “simple” capping and stabilizing agents as in the organometallic precursor decomposition reactions.

The gold colloid was prepared at room temperature using a didodecyltrimethylammonium bromide (DDAB)/water/toluene inverse micelle system^[40]. Through controlling the amount of surfactant, water, reducing agent, gold salt, the rate of reaction and the reaction temperature, inverse micelle synthesis usually produces nanoparticles with the average particle size depending somewhat on the size of the micelles. The prepared gold nanoparticles have a wide size distribution, from tiny particles as small as 1 nm to very large particles with the size of 80 nm. The large size distribution was apparently caused by the homogeneous growth of the nanoparticles due to the low DDAB concentration. After stirring of prepared colloid with dodecanethiol, the color of the colloid turned from dark red to slightly purple. Dodecanethiol has a strong affinity to the gold surface^[41] which results in a change of the interaction strength between the particles. The purple color was caused by the aggregation of the gold particles^[42]. The color of the colloid changed back to red within a minute during the refluxing which indicated a non-aggregated state of the particles in the colloid. The ligand modification and reflux digestion caused a dramatic improvement of particle size distribution. The amount of dodecanethiol also affected the final size of the system. If an extra dodecanethiol was added to colloid, a much larger particle size was observed after 3 h of digestion, with average size of 8.7 nm. Therefore a large amount of extra dodecanethiol molecule is needed for this complete digestion to occur. The amount of water existent in the reaction precursor also influenced the final particle size after digestion. As the amount of water in the DDAB/water/toluene system was increased by several times, the prepared sample is also very polydisperse with a significant amount of very smaller particles with diameter 3–4 nm. One possible explanation is the increased water concentration allows more nucleation sites in the system. By sharing materials between these nucleation sites, the overall particle size after digestion decreases. Long time digestion (up to 12 h), however, did not seem to further narrow the particle size distribution.

Djalali et al. have reported a novel method to produce gold nanoparticles in soft templates (doughnut-shaped nanoreactors), peptide nano-doughnuts^[43]. The nano-doughnuts were self-assembled from peptides and organic gold salts. Various shapes of peptide/protein assemblies have been produced in biomaterials^[44]. Monodisperse gold nanocrystals (AuNCs) grew

inside the cavities of peptide nano-doughnuts by the reduction of Au ions trapped in the cavities and the resulting AuNCs were extracted by destroying the nano-doughnuts via long UV irradiation [Figure 3]^[45]. Because the peptide nano-doughnuts already contained gold ions inside the cavities, Au nanocrystal synthesis was completed in a simpler process as compared to that of micelle nanoreactors. Those features may allow peptide nano-doughnuts to be applied in the fields of nanomaterial syntheses, controlled release systems, and drug delivery. When the peptide monomers were self-assembled in the growth solution without the organic gold salts, peptide nanotubes were formed instead of the peptide nano-doughnuts^[46]. Those nanotubes were assembled via intermolecular hydrogen bonds between amide and carboxylic acid groups. Therefore, the addition of the organic gold salts to the peptide monomer assembly likely has a significant influence on those chemical interactions to alter the assembled structure. Because the nano-doughnuts were not observed when an inorganic gold salt, HAuCl_4 , was incubated in the peptide solution instead of AuPMe_3Cl , the ligand of this organic gold salt may play an important role in the assembly of the nano-doughnuts. The IR investigation suggests that the organic gold salts are incorporated in the peptide self-assemblies and contribute to the nano-doughnut formation. The amide peak shifts were observed in amide-containing self assembled monolayers, after gold salts were bound to their amide groups^[47]. When the peptide nano-doughnuts were weakly reduced by UV irradiation in 20min, gold nanocrystals were observed inside the doughnut cavities. The particles in the center of the doughnut cavities are identified as gold nanocrystals from the SFM phase images, the TEM images, and the electron diffractions. In fact, the incorporation of the gold nanocrystal increases the mechanical strength of the peptide nano-doughnut. After those samples were dried on mica surfaces, the peptide nano-doughnuts without gold nanocrystals collapsed and displayed a deformed ring shape, whereas the peptide nano-doughnuts with gold nanocrystals inside the cavities showed a monodisperse and isotropic ring shape.

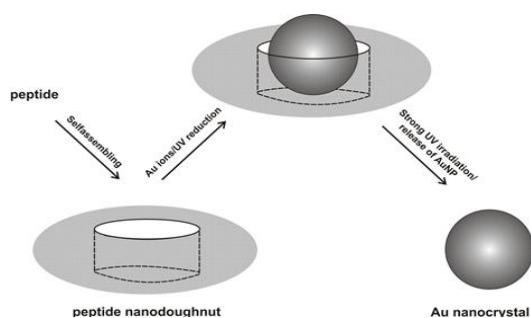


Figure 3. Scheme for the peptide nanodoughnut formation^[45].

A solid phase place exchange reaction can be also used to synthesize gold nanoparticles with monofunctional group attached to the surface^[48]. This approach is based on a “catch and release” mechanism. Bifunctional thiol ligands with a carboxylic end group were first immobilized on a solid support such as a polymer resin with a controlled density. The density was low enough that neighboring thiol ligands were far apart from each other. When the modified polymer support was incubated in a butane thiol protected gold nanoparticle solution, a one-to-one place exchange reaction took place between the polymer-bound thiol ligands and the nanoparticles. After cleaving off from the solid support, nanoparticles with a single carboxylic group were

obtained as the major product. Jacobson et al. published an almost identical approach toward the synthesis of gold nanoparticles with a single amino acid moiety^[49]. These nanoparticles with a single functional group attached can be treated as giant “molecules” and linked together into very sophisticated structures through traditional chemical reactions, just like the total synthesis of complicated natural product from small molecular units.

Silver nitrate aqueous solution was directly used to prepare silver nanoparticles in sodium bis(2-ethylhexyl) sulfosuccinate (AOT)–dodecane–water–silver nitrate–hydrazine hydrate microemulsions^[50]. The silver nanoparticles were obtained from the reduction of silver nitrate by hydrazine hydrate. It is found that the particle mean diameter decreases significantly with increasing silver nitrate concentration when silver nitrate concentration is less than or equal to 0.2M. However, it increases when silver nitrate concentration is greater than 0.2M, that is, with increasing AgNO_3 concentration the growth rate of the silver particles is more rapid, and the particle size decreases until an optimum amount. After the optimum amount, the particle size increases again. When silver nitrate concentration is greater than or equal to 0.4M, the silver colloid is unstable and easy to flocculate. TEM data indicate that there are fewer but larger silver nanoparticles generated in the microemulsion formed by 0.1M silver nitrate ($d=3.93\text{nm}$). By contraries, there are more but smaller nanoparticles performed in the microemulsion formed by 0.2M silver nitrate ($d=2.6\text{nm}$), which means that the higher the silver nitrate concentration, the faster the growth of nanoparticles. Thus, the tiny particles are easy to aggregate into larger particles at the high silver nitrate concentration due to the weakened adsorption of AOT molecules on the particles’ surface. Besides TEM micrograph, these conclusions have also been confirmed by the UV–vis spectra^[51]. The primary study shows that the absorption intensity increases with increasing AgNO_3 concentration, which reflects the formation of more silver nanoparticles. At low concentration of AgNO_3 , the maximum absorption wavelength gives rise to a blue shift, meaning a decrease of the particles size. At high concentration of AgNO_3 , the maximum absorption gives rise to a red shift, meaning the particles size increased^[52] and the large silver aggregates formed. TEM micrograph and size distribution histogram of silver colloidal (diameter) particles obtained at various ω ($= [\text{water}]/[\text{surfactant}]$) values:

$$d(\text{nm})/\omega : 1.52/2.5, 3.39/7.5, 4.98/15.0$$

It was reported that the particles are spherical in shape and there is narrower in the size distribution at lower water content than that obtained at higher ω values. Hence, a decrease in the micellar size, i.e., a decrease in the molar ratio of water to AOT, induces formation of smaller and more monodisperse silver nanoparticles. Because at low water content the water solubilized in the polar core is bound by the surfactant molecules, which increases the boundary strength and decreases the inter micellar rate among the reverse micelles. Hence, a decrease in the water content induces formation of monodisperse silver particles with smaller diameter size. Increasing the water content, the bound water turns into bulk water, which is benefit for the water pools to exchange their contents by a collision process and make the chemical reaction or coprecipitation between compounds solubilized in two different reverse micelles more easily.

Thus, reactants can be rapidly transferred from one water core to another. As a result, the rate of nucleation and the particle growth begin to be controlled by the collision, fusion and split of the droplets. Due to the nature of bulk water drastically different from bound water, the resultant particle size is relatively bigger and the size distribution is commonly wider.

Other Nanoparticles

The first report on the synthesis of platinum nanoparticles of different shapes (tetrahedral, cubic, and truncated octahedral)^[53] appeared in 1996. Recently, there has been a lot of interest in the synthesis of platinum nanoparticles of different shapes such as tetrahedral^[53], cubic^[53,54], nanowire^[55], tetrapods^[56], etc. A modified version of the hydrogen reduction method using the polyvinylpyrrolidone (PVP, $M_w = 360000$) and the potassium hexachloroplatinate precursor salt has also been developed to prepare tetrahedral platinum nanoparticles^[57]. Cubic platinum nanoparticles capped with oxalate have also been prepared using the hydrogen reduction method^[54]. Modifications of the discussed hydrogen reduction methods^[57] have been used to prepare PVP capped tetrahedral platinum nanoparticles^[58]. In addition, modification of the hydrogen reduction method^[53] has been used to produce polyacrylate capped cubic platinum nanoparticles^[59]. Platinum nanowires, tetrapods, and “sea urchins” have been synthesized using different modifications of the ethylene glycol reduction method and PVP as the capping agent^[56].

The tetrahedral platinum nanoparticles are synthesized by making modifications to the hydrogen reduction method^[57] and are capped using the polyvinylpyrrolidone polymer^[60]. The cubic platinum nanoparticles are also synthesized by making modifications to the hydrogen reduction method^[53] and are capped using the polyacrylate capping agent^[61]. The spherical platinum nanoparticles are synthesized using the ethanol reduction method^[62] and are capped using PVP. The dominantly tetrahedral nanoparticles have an average size of cap 4.8 nm, the dominantly cubic nanoparticles have an average size of 7.1 nm, and the dominantly spherical nanoparticles have an average size of 4.9 nm^[60, 63].

The effect of emulsifier type and temperature on the kinetics of the formation of platinum nanoparticles in water(w)/heptane(o) microemulsions by chemical reactions of PtCl_6^{2-} were examined with time resolved UV-V is absorption spectroscopy^[64]. The surfactant used were poly(ethylene glycol) monododecyl ethers (C_{12}E_4 (Brij 30), C_{12}E_5 , C_{12}E_6), AOT, mixtures of the alcohol ethoxylates and AOT and the reducing agent NaBH_4 . Since reduction of PtCl_6^{2-} by diffusion of BH_4^- through the oil continuous domain is rather unlikely, the fusion of droplets is a prerequisite for the reaction to proceed and may be the rate-determining step in the reduction of PtCl_6^{2-} to metallic platinum. Alternatively, the difference in rate of particle formation may be due to a difference in the microenvironment within the fused water droplets of the microemulsion that form after mixing of the two reactant systems. The rate of droplet fusion is likely to be governed by the type of emulsifier that forms the palisade layer at the oil-water interface. However, it is not self-evident which of the two types of emulsifiers, AOT or an alcohol ethoxylate, would give the highest rate of fusion. The anionic emulsifier AOT is much less soluble in the continuous hydrocarbon domain than the nonionic emulsifiers used. The high solubility of the alcohol ethoxylate in the continuous domain will lead to a flux

of emulsifier molecules back and forth between the bulk hydrocarbon domain and the droplets interface. This process will work against tight and ordered packing of alcohol ethoxylate and can consequently be expected to favor droplet fusion. In contrast, the water droplets stabilized by AOT can be regarded as hard spheres, which may lead to more elastic collisions and slower rate of fusion of droplets^[65]. The platinum particles were found to be less than 5 nm in average diameter, which was consistent with the microemulsion droplet size.

It is also conceivable that the difference in kinetics between the AOT and the nonionic based microemulsions is related to differences in the emulsifier's ability to act as ligand in the platinum complex. Shelimov et al^[66] suggested several different mechanism for the interaction between PtCl_6^{2-} and alumina, e.g., electrostatic adsorption of the hexachloroplatinic complex at the alumina surface and ligand substitution reactions, where alumina surface groups replace some the initial ligands in the chloroplatinic complex. In the latter case, both OH-bridging ligands and Cl-bridging ligands are suggested. One can envisage ways in which the emulsifier head groups, both polyoxyethylene chains of nonionic surfactants and the sulfonate group of AOT, can interact with the platinum in the hexachloroplatinic complex. The interaction will differ depending on the type of surfactant, and the difference in binding between Pt and the ligands in the complex may influence the kinetics of the reaction inside the droplets.

Colloidal Pt was also synthesized by reducing H_2PtCl_6 with hydrazine in w/o microemulsions consisting of C_{12}E_4 (Brij 30), n-heptane and water^[67]. The authors reported the optical properties of nanosized (≈ 4 nm) Pt particles and related their optical properties to the kinetics of the reaction carried out in their preparation. The absorption spectrum of H_2PtCl_6 in the microemulsion shows two different bands, one centered at 220 nm and the other at 260 nm. When the microemulsion with the reducing agent is added to the microemulsion containing H_2PtCl_6 , these bands disappear, and a new peak centered at 236 nm, the only peak in the absorption spectra appears. These results can be explained by assuming that two different steps are involved during the formation and stabilization of the particles. In the first step, the particles are formed inside the aqueous droplets and the adsorption band (220 nm) lies very near to the theoretical band position in water (215 nm)^[68]. In the second step, some kind of interaction between the particles and the reactants causes the displacement of the observed band to 236 nm. The band that appears in the optical spectra of Pt in microemulsion, when the salt reduction has been completed, is caused by the electronic surface excitation due to the electric field of the incoming light. Microemulsions containing only Pt salt were exposed to daylight for several days, and only after more than one month small changes in the spectra were measurable. But when microemulsions are exposed to daylight and kept at the same time in a thermostatic bath at 50°C, the process is strongly accelerated, and a typical brown color appears after only few minutes. Barnickel et al^[69] have reported that the terminal hydroxyl groups of the C_{12}E_5 surfactant are capable of reducing Ag^+ ions upon radiation. To check this hypothesis, Rivadulla et al^[67] tried to obtain Pt by keeping samples at different temperatures with/without exposure to light irradiation but changing the system to AOT/n-hexane/water, because in this surfactant there are no terminal hydroxyl groups. Very small changes were observed

at room temperature. At 50°C the reaction produces a typical brown color which appears after few minutes. The reactions are catalyzed by exposure to daylight, but the reaction is strongly dependent on the temperature due to the chemical reduction by the surfactant molecules. After 48h at 50°C the microemulsion shows a spectrum identical with that observed by Pt particles obtained by hydrazine reduction, confirming the formation of colloidal Pt particles without reductant addition. As the heads of the ionic surfactant AOT are composed of sulfonate groups, the reduction can be explained by assuming that the electronic pairs of the oxygen in the sulfonate group donate the electrons, causing reduction during irradiation, such as the oxygen of the hydroxyl groups of the $C_{12}E_5$ molecules. Colloidal Pt was obtained without hydrazine by heating and daylight exposure. Furthermore, the impurities in AOT can also take part in the reduction mechanism^[70]. The optical properties of the metallic particles are identical with properties of the corresponding particles prepared with hydrazine.

Zhang and Chan have reported the synthesis of bimetallic Pt-Ru nanoparticles using a reverse microemulsion of water/Triton X-100/propanol-2/cyclohexane^[71]. Platinum-ruthenium nanoparticles were formed upon contact between the precursor containing droplets and the hydrazine containing droplets. Two plateaus of particle sizes 2.5 and 4.5 nm (determined by TEM) appear at low and high metal salt concentrations:

$$d(\text{nm})/([\text{Ru}] + [\text{Pt}])\text{mM}: 2.5/6, 2.6/10, 2.6/20, 4/40, 4.5/60, 4.6/100$$

The particle size was around 2.5 nm and unaffected by the Pt-Ru concentration when it was below 20 mM. When the Pt-Ru concentration was above 20 mM, the size of Pt-Ru nanoparticles increased with the metal salt concentration until 60 mM, beyond which the average nanoparticle size remained at 4.5 nm. This size dependence on concentration of precursor was similar to that reported^[72] for nickel nanoparticles prepared from NiCl_2 and hydrazine with a cationic surfactant.

The hydrodynamic diameter (d_{droplet}) of the hydrazine microemulsion droplets was 1.62 nm, whereas that of Pt-Ru complex varies from 26 at 2 mM Pt-Ru to 83 nm at 100 mM Pt-Ru:

$$d_{\text{droplet}}(\text{nm})/([\text{Ru}] + [\text{Pt}])\text{mM}: 26/2, 28/6, 26/10, 29/20, 41/40, 56/60, 83/100$$

A minimum size of 2.5 nm was required to overcome the surface energy during nucleation of a Pt-Ru nanoparticle. For precursor concentrations below 20 mM, several Pt-Ru droplets are required to form a nucleus, and collisions with a stoichiometric number of hydrazine droplets are also required. Beyond 20 mM, a single precursor droplet contains Pt-Ru beyond the nucleation limit, and growth can occur upon the entrance of hydrazine droplets. It should be emphasized that the probability of collision among Pt-Ru-containing droplets is very low because at 40 mM, they are outnumbered by the hydrazine droplets by a factor of >104. It is also known that mobility of a larger colloid decreases with size. The control of size distribution can be achieved by using low metal concentration or decreasing the size of the microemulsion droplets containing the metal complex by improving surfactant and microemulsion parameters.

Palladium nanoparticles were obtained from a novel

type reverse microemulsion of Bis (N-octylethylenediamine) palladium (II) chloride, water and chloroform ($[\text{Pd}(\text{oct-en})_2]\text{Cl}_2$ /water/ chloroform) using NaBH_4 as a reducing agent^[73]. Relatively uniform-sized particles were obtained from 0.025 or 0.05 mol kg^{-1} $[\text{Pd}(\text{oct-en})_2]\text{Cl}_2$ in chloroform solution at [water]/ $[[\text{Pd}(\text{oct-en})_2]\text{Cl}_2]$ (ω) = 7.6. Under this condition, twice moles of free oct-en ligands for the Pd complex were added to stabilize the reverse micelles. At $\omega > 20$, the water/ $[\text{Pd}(\text{oct-en})_2]\text{Cl}_2$ /chloroform microemulsions without cosurfactant were obtained. At $\omega = 50$ the TEM picture showed an onset of the bicontinuous structure. At $\omega < 10$, the structure of the aggregates is surely a droplet-type reverse micelle. In the system A ($\omega = 7.6$, $[\text{oct-en}] = 0.2$ mol kg^{-1} , $[\text{Pd}(\text{oct-en})_2]\text{Cl}_2 = 0.05$ mol kg^{-1}), the palladium particles are relatively uniform-sized and the sizes are smaller ($d_p = 4.2$ nm). In the system B ($\omega = 50$, $[\text{Pd}(\text{oct-en})_2]\text{Cl}_2 = 0.5$ mol kg^{-1}), the spherical domains of the w/o microemulsion s are still present even when the structures of larger domains are close to the bicontinuous phase at $\omega = 50$ and at a larger palladium concentration. The size and its deviation are somewhat larger compared to those at $\omega = 7.6$, where the water pool is a droplet type. It is coincided with a result that the metal particles become smaller at a lower original metal concentration^[74]. In the presence of methanol the shape of the palladium particles is significantly deformed from the spheres. The water/ $[\text{Pd}(\text{oct-en})_2]\text{Cl}_2$ /chloroform system has two characteristic features. Firstly, the highly condensed palladium nanoparticles were obtained by using the novel type double-chain palladium complex. This result is attributed to the high concentrations of the palladium (II) ions in the water domains of the present aggregation systems. Secondly, the structures of the aggregates of the original palladium complex surfactants were directly reflected in the shapes of the palladium nanoparticles because of the palladium being located in the head group of the original metal complex surfactant. In the alkylethylenediamine system, the palladium complex surfactant acts as both a metal ion provider and a metal particle stabilizer: it is a rare case. As the alkylethylenediamine has a capacity to form metal complexes with various transition metals, this method will be universally applicable to obtain metal nanoparticles in high yield.

Ripening Processes

The polydisperse reaction dispersions can be accompanied by the degradation of nanoparticles. Under such conditions the large particles growth on the expense of the small ones. This growth phase is called Ostwald ripening^[75,76]. In this process the high surface energy of the small particles promotes their dissolution and the dissolved material is then re-deposited on the large particles. The decreased fraction of smaller particles can lead to the increase of particle uniformity. The ‘‘Ostwald ripening’’ process involves ‘‘the growth of larger particles (crystals) from those of smaller size which have a higher solubility than the larger ones’’^[77]. In their preparative solution, for example, a group of free standing crystallites with unequal sizes in non-equilibrium form will further differentiate and redistribute themselves through the above solid-solution-solid process to achieve a more uniform size distribution [Figure 4].

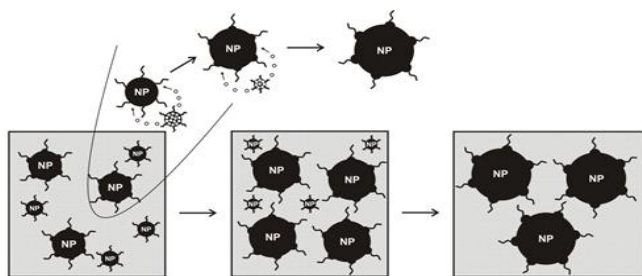


Figure 4. Oswald ripening process^[77].

The narrow size distribution of the particles is achieved by the remarkable procedure of “digestive ripening”^[78]. This simple procedure is based on the reflux of a polydisperse nanoscale colloid for a certain amount of time, resulting in a dramatic improvement of the size distribution of the particles. The formation of gold monodisperse nanoparticles nano crystals through a novel digestive ripening process and a temperature dependent size segregation process was reported by Lin et al^[40]. The authors^[40] demonstrated a simple and straightforward approach to obtain narrow size distribution gold nanoparticles from a very polydisperse colloid by ligating the nanoparticles with dodecanethiol followed by a digestive ripening process. Temperature induced size segregation can be used to further select the desired particle size.

Stoeva et al. have applied the digestive ripening process for the formation of a monodisperse colloid from the polydisperse gold-toluene-thiol colloid and discussed the mechanism of particle variations^[79]. The procedure involves heating under reflux of a gold-toluene-thiol colloid. A polydisperse colloid containing particles with sizes ranging from 1 to 40 nm is transformed into an almost monodisperse colloid with particle sizes of about 4-4.5 nm. The UV/vis absorption spectrum of the colloid after cooling to room temperature shows an appearance of a definite plasmon absorption maximum at 513 nm, which is in agreement with the size and monodispersity of the obtained particles. The UV/vis absorption spectrum of colloid 2 is in agreement with the sizes of the particles observed in TEM. It is characterized by a broad plasmon absorption band with no definite maximum^[80].

Heating of gold-toluene-thiol colloid under reflux results in a dramatic narrowing of the particle size distribution^[81]. TEM studies of a hot colloidal solution show formation of spherically shaped particles with sizes of about 4 nm. They have a tendency to organize into 2D layers. Some of the particles from the hot colloid organize in nice 3D structures. The remarkable effect of the digestive ripening procedure is the great improvement of the size distribution. The amazing result is that the particles predominantly organize on the TEM grid in large 3D structures in only about 15 min after the digestive ripening process is finished. A small number of areas of 2D arrangement are also observed. Even larger 3D structures (>3 μm) are observed after 1 day. The results suggest that the activation energy for 2D organization is lower compared to that of 3D organization. Of course, one of the most interesting features of the synthetic sequence reported herein is the digestive ripening step, and the mechanism for this remarkable process is not entirely clear. Only a few useful facts are known. First of all, nanoparticles are the necessary starting material; that is, normal gold powder is not susceptible to digestive ripening, showing again that nanosized particles are intrinsically more chemically reactive than bulk samples^[82].

Functionalization

The ligand exchange reaction is an extremely versatile tool for the preparation of functionalized metal nanoparticles^[83]. This method is fast and simple to use; it allows one to introduce functional groups that are incompatible with other methods for nanoparticle synthesis. A report by the R. W. Murray group suggests a new role of reaction conditions in mediating the exchange reaction^[84]. It was demonstrated that triphenylphosphine (TPP)-stabilized gold nanoparticles^[85] undergo ligand exchange reactions with a few ω -functionalized thiols to produce functionalized nanoparticles that preserve the core dimensions of the precursor particles but exhibit highly increased stability against heat, aggregation, and decomposition^[86].

Colloidal noble metal nanoparticles have received much attention as supporting scaffolds, decorated with functional units that allow their use in sensors and devices^[87]. The strong interaction between n-alkylthiols and the gold surface provides the most popular method for the attachment of molecular groups^[88]. Such bonding is convenient to engineer, but is reversible at moderate temperatures and kinetically unstable with respect to movement of thiols on the surface^[88]. Thus, groups that are deposited onto a metallic surface cannot be precisely fixed with respect to one another, although average spacing can be arranged by diluting the monolayer of functionalized alkylthiols with analogues lacking the functional group^[89]. Precise, angstrom level control of reactivity in nanotechnology requires nanoscale building blocks of known structure at atomic resolution.

The passivation of gold particles with acetone leads to the gold-acetone (colloid 1) which has a brown color, particles well-dispersed in solvent and particles ranging from 10 to 50 nm in pure acetone solvent^[81]. The addition of toluene changes the color of the gold-acetone-toluene-thiol colloid to a dark brown color (colloid 2). TEM studies of this colloid show particles ranging from 5 to 40 nm with no definite geometrical shapes^[79]. Both stabilization (steric and electrostatic) processes take place during the warm up step, which has to be carried out slowly in order to ensure good stabilization. Gold-toluene-thiol colloid (colloid 2) was obtained by vacuum evaporation of all the acetone from colloid 1. Drastic change of the size and shape of the particles is characteristic at this stage. Nearly spherical particles with sizes in the range of 1-6 nm are dominant. There are also a small number of larger particles (10-40 nm) like those in the initial acetone containing colloid (colloid 1). One possible explanation for the change of size and shape of the gold particles induced by the removal of acetone is due to the change in interaction particle solvent. In colloid 1 the amount of acetone is in great excess. In great excess of acetone the gold particles are strongly solvated by acetone and the attachment of dodecanethiol (RSH) molecules on the particles surface is suppressed. Acetone, with its nonbonding electron pairs, can serve as a reasonably good ligand for gold but can only compete with RSH at high acetone concentrations. Therefore, as acetone is removed, the thiol competes better and better. This effect would be enhanced by the fact that the long-chained thiol is less soluble in acetone than in toluene. Acetone acts as a preliminary stabilizing agent, which is substituted by dodecanethiol molecules when acetone is evaporated. This ensures good dispersity of the thiol-ligated gold particles in the toluene medium. In addition, toluene is anticipated to achieve much better wetting of the thiol

molecules on the gold particles surface compared to the more polar solvent acetone. In favor of this are results obtained for the wetting of undecanethiol self-assembled monolayers on gold surface by water and hexadecane^[90]. It was found that hexadecane as a nonpolar solvent wetted the thiol molecules on the gold surface much better compared to water^[90]. It is reasonable to expect a similar wetting trend for acetone, hexane, toluene, etc. due to their different polarities.

Although gold nanoparticles can be prepared from various materials by several methods^[91], the coupling and functionalization with biological components has only been carried out with a limited number of chemical methods. To apply gold colloids in newly developed biomodifying medical assay systems, a simple and facile means of anchoring different ligand biomolecules onto particle surfaces are strongly required as well as the stability in the physiological condition should be improved. Particularly, color changes induced by the association of nanometer sized gold particles provide a basis of a simple yet highly selective method for detecting specific biological reactions between anchored ligand molecules and receptor molecules in the milieu. Colloidal noble metal nanoparticles, in particular, have found application in a variety of assay formats in which analyte binding is coupled to particle adsorption. With decreasing gold colloidal particle size, however, colloidal stability decreases significantly due to increased particle surface energy. Such gold nanoparticles aggregate in high ionic strength milieu as well as adsorb biomolecules, resulting in reduced sensitivity and selectivity when used as colloidal sensor systems in biological fluids. Functionalization of gold nanoparticles involves the use of functional ligands in which a moiety is used for anchorage to the particle while the other is directed to the outer-surface for specific interaction with biomolecules. For example, thiol-modified oligonucleotides have been used to functionalize AuNPs for specific detection of nucleic acid sequences in biological samples. Functionalization of AuNPs with biomolecules other than nucleic acids has also been used in order to develop methodologies suitable for clinical diagnostics. These include: 1) antibodies for signal enhancement in immunoassays^[92]; 2) carbohydrate functionalization to study specific molecular interactions^[93]; and 3) surface functionalization with ligands that can be tailored for specific protein binding^[94] or direct binding of peptides and proteins to the Au-nanoparticle surface^[95].

Thiol-Stabilised Gold Nanoparticles

The first report of thiol-stabilised gold nanoparticles appeared in 1993. In this study by Giersig and Mulvaney^[96], gold particles prepared as hydrosols were capped with alkane thiols to render them soluble in a non-polar solvent. They were found to form two-dimensional hexagonal super lattices in a fully reversible deposition process. In addition to this remarkable finding it was reported that the inter particle spacing was to some extent adjustable with molecular precision by the choice of alkane thiol ligands of different chain length. Detailed studies of particle shape^[97] revealed that the truncated cuboctahedron is the predominant structural motif, but other geometries such as dodecahedra, dodecahedra and icosahedra are typically also present in the same preparation. However, not all types of thiol ligands lead to the same extraordinarily high degree of stability that can be achieved by the use of alkane thiols with a hydrocarbon chain length of C₅ to C₁₈. The other simple method was reported to in-

duce super lattice formation directly in a slightly polydispersed gold colloid by modifying the nanocrystal surface with certain ligands^[98].

A range of different monolayer patterns were observed when the gold colloid was treated at higher temperature in order to decrease the level of pure toluene in the continual solvent phase (the residue thiol volume fraction in these colloids was less than 5×10^{-4})^[99]. With pure toluene solvent, the liquid film may thin enough before the nucleation limit is reached so that dewetting from the substrate occurs before super lattice formation. When the particle concentration was increased, the pattern morphology changed from small isolated domain structures to percolating domains and eventually to compact domains. These different structures are frequently seen in the literature as well^[100]. Dewetting causes holes to open up in the liquid layer and particles to move outward, away from the holes, as the liquid evaporates. On the other hand, convective flow inside wetting droplets has the tendency to drive the particles in the opposite direction^[101]. Only when the interactions between particles and the substrate and between particles are strong enough will the nano crystals (nanoparticles) be pinned to the substrate. The domains thus formed depend on the nano crystal concentration. Isolated domains of nano crystals form at low particle concentration when the pinning effect is weak and dewetting holes percolate across the substrate. As the particle concentration increases, the pinning effect becomes stronger because of the increase frequency of particle interactions. Dewetting holes then become more isolated and percolating particle domains form. At an even higher particle concentration, the sizes of the dewetting holes decrease significantly and a more compact monolayer is formed. In addition to the effect of dewetting, a AFM study^[102] has shown that the inter particle interaction might become strong enough to cause spinodal phase separation during the liquid drying process. This effect would also cause particles to form percolating domains. Despite the strong pinning effect and the entropy-driven ordering tendency in the case of high particle concentrations, local disorder and voids are still inevitable in a compacted monolayer. Further increasing the particle concentration does not improve the monolayer ordering significantly before bilayer formation starts to appear. To maintain a wetting layer on the surface so that nano crystals can have a chance to self-assemble into large periodical structures, the evaporation rate of the solvent must be slowed.

Dodecanethiol ligand was used to modify the surface of the gold nano crystals. The change of electron density on the particle surface and the change of adjacent environment by the ligand increase the attractive interaction between nano crystals^[78]. After they were reflux heated in the presence of dodecanethiol, all the samples kept at temperatures higher than 80°C showed no sign of super lattice or other types of aggregate formation, because the increase of the free energy due to the ordering (entropy loss) is much larger than the lowering of the free energy from bringing particles into close contact. On the other hand, samples kept at temperatures lower than a certain critical temperature became supersaturated and nucleated into aggregates that have super lattice structures. The critical temperature depended on the concentration of the colloid. The nano crystal super lattice (NCS) structures gradually aggregated together to form fractal like aggregates and settled down to the bottom of the vial (at 60°C and gold nano crystal concentration of 0.24×10^{-6} M). The

top layer of the samples that contained NCS appeared red after being left undisturbed for a couple of days. TEM showed that this top layer contained mainly single nano crystals. The formation of gold NCSs from colloidal nucleation resembles the formation of molecular crystals from a saturated solution. The nucleation process of NCS depends on both the concentration and the temperature of the single nano crystal colloid. Samples synthesized with different gold concentrations were compared at different temperatures. Colloids containing NCS appear to be purple and colloids without NCS formation are red. A phase boundary between single nano crystal colloids and NCS colloids clearly exists. Super lattices formed at 60°C were roughly 3 times the size of the super lattices formed at 23°C. The difference in super lattice size was attributed to the formation of a different amount of nucleation sites when the reflux heated samples were cooled to the two temperatures. For $0.24 \times 10^{-6} \text{M}$ colloids, 60°C is only slightly below the phase boundary; therefore, colloids quenched to this temperature had fewer nucleation sites and each nucleation site subsequently grew into a large size of super lattice. In comparison, colloids quickly quenched to 23°C resulted in large number of nucleation sites and the simultaneous growing of all these sites result in smaller size of super lattices^[78].

The formation of micron size particles in an ordered array has been known for a long time^[103]. It relies on the balance between the long range van der Waals interaction, sometimes called the Hamaker interaction, and the repulsive electrostatic and steric interactions^[104]. These interactions are described in detail by the DLVO theory^[105,106], which predicts a second minimum, usually beyond 3 nm from the primary energy barrier. The micron size colloidal particles can be relatively stable when they reside in this second minimum well^[107]. The formation of nanocrystal super lattices from the colloid, on the other hand, requires a much more delicate balance between the attractive force and the repulsive interaction. This is due to the fact that nano crystals have a much smaller second minimum in the potential curve as compared with micron size particles^[108]. For the same reason, these super lattices can be easily dissolved upon heating the colloid. At room temperature, the colloids containing NCSs appeared purple, with a broad absorption band extended to the long wavelength of the visible region. As the sample was heated, it crossed the phase boundary and the color of the colloid gradually changed to red, with the absorption spectra eventually changed to the single nanocrystal surface plasmon absorption at around 530 nm.

Thiol-stabilized gold nanoparticles have not only been used as building blocks for larger structures comprising hundreds or thousands of particles but are also of interest as individual large molecules, i.e. so called monolayer protected clusters (MPCs)^[88]. They represent nanoscopic metal surfaces and can be regarded as three-dimensional analogues of two-dimensional macroscopic surfaces. The preferred structures of larger gold clusters comprised of 100 to 1000 atoms (1.4–3.0 nm equivalent diameter) have been determined theoretically via exhaustive search and energy minimization methods and experimentally by synchrotron x-ray diffraction analysis of purified powder samples of small gold nano crystals passivated by alkylthiol (ate) self-assembled monolayers^[97].

A great deal of relevant information is available on the packing and energetics of the alkylthiol (ate) monolayers on gold, particularly from the simulations^[109], and generally

because these are the nanocrystal analogs of the exceedingly popular noble-metal thiolate self-assembled monolayer (SAM) surface systems^[41]. The properties of such $\text{Au}_n(\text{SR})_m$ assemblies, and for planar surfaces, include that the surfactant head groups form a compactly packed mantle surrounding the core, with ratios of S to surface Au atoms in the range of 1:2 to 1:3, depending on the exposed facet, but somewhat higher in 1.5-2.5 nm diameter nanocrystals; and that the adsorption (desorption) energy^[110] see also^[111] of ~ 1.3 eV per dimeric RSSR molecule (dialkyldisulfide) adsorbed thus is small (< 0.3 eV per surface gold atom) compared to the cohesion of gold (3.9 eV per atom) and comparable to the unusually low surface energy of gold (ca. 0.4 eV per surface atom), consistent with minimal disruption of the gold surface structure and a probable S-Au bonding mode involving only the nonbonding electrons of an intact RSSR molecule^[112]. Although this reduction in the surface energy is relatively small, it does point to one clear mechanism by which the lattice contraction is reduced. Further, since this surface energy lowering is facet-type dependent, it reduces the cost of (100) facets more than that of (111) facets, its net effect may be an earlier than expected stabilization of the single-crystal forms, including their twins.

The further step towards more complex structures is to control the linkage of particles to each other or to the surface of an already existing structure. The simplest approach to such systems is to allow the particles to react with bifunctional molecules which can attach to the surface of two particles and link them together. This has been demonstrated for alkane dithiols, which can be used, for example, to precipitate cross-linked networks of gold particles from solution^[113]. The highest degree of control in the self-assembly of nanoparticle structures reported so far is achieved by exploiting DNA base pair recognition^[114]. The DNA/nanoparticle conjugates can then recognize complementary DNA sequences and bind them with extremely high selectivity. In this way it has been possible to bind particles to each other and to surfaces in a controlled fashion. Geometries such as lines of several particles along a DNA strand, as well as doublets and triplets of particles joined by DNA, have been produced.

It was observed that the hysteresis in the π -A isotherms is small immediately after the spreading of the monolayer of hydrophobized gold nanoparticles ($t=0$) and that the hysteresis increases steadily with time stabilizing after 12h of the spreading of the monolayer^[115]. The sum of the gold core (given by TEM) and the length of the laurylamine molecule led to the estimation of the area per particle to be ca. 85 nm². This limiting area is much smaller than the closest packing area of ca. 350 nm²/cluster observed in the π -A isotherm measurements. One possibility of the difference is repulsive electrostatic interactions between gold particles, which would be sufficiently long range to account for the large takeoff areas observed. It is possible that the gold nanoparticles consists of a positive charged core that is masked by the hydrocarbon sheath, rendering it hydrophobic. Another important observation is the increase in takeoff area with time. This is suggested to be due to reorganization of the octadecanol molecules in the monolayer with time scales that are relatively slow. One mode of reorganization could be interdigitation of the hydrocarbon chains in octadecanol and laurylamine molecules. This process would lead to a very large tilt in the orientation of the octadecanol molecules and consequently, an increase in the monolayer area. Langmuir monolayers of just the lauryl capped

gold nanoparticles did not yield stable monolayers on the surface of water. While monolayers of the laurylamine capped gold nanoparticles at the air-water interface were not amenable to layer-by-layer transfer onto solid supports, it was observed that addition of the water insoluble amphiphilic octadecanol to the gold nanoparticle solution improved the stability of the monolayer at the interface as well the multilayer assembly protocol.

Fendler and co-workers first demonstrated that surface-modified hydrophobic colloidal nanoparticles may also be organized at the air-water interface more specifically, on the surface of water and that multilayer films of the nanoparticles could be formed on suitable substrates by the LB technique^[116]. A number of other groups have now used this method to form multilayer films of gold particles^[117], polymer-capped platinum colloidal particles^[118], bulky balls^[119]. The Brust synthesis procedure^[7] wherein gold nanoparticles are synthesized and capped with alkanethiols in a nonpolar organic phase continues to be the most popular means of obtaining hydrophobic gold nanoparticles that are readily dispersible in different non-polar/weakly polar organic solvents^[120]. It was demonstrated an alternative method for obtaining hydrophobic gold nanoparticles synthesized in water by electrostatic coupling with fatty amine molecules present in nonpolar organic solvents^[121]. The process consists of vigorous stirring of a biphasic mixture of aqueous colloidal gold particles and a nonpolar organic phase containing alkylamines such as octadecylamine^[121]. During the stirring process micro droplets are formed that enable binding of the alkylamine molecules with gold nanoparticles thereby rendering them hydrophobic and soluble in the organic phase. The alkylamine-stabilized colloidal gold particles could be separated out in the form of a powder and dissolved in different organic solvents^[121]. A linear increase in the absorbance intensity with number of monolayers of laurylamine gold nanoparticles in the LB films indicating that excellent layer-by-layer transfer of the hydrophobized gold nanoparticles had occurred. This result, together with QCM results, clearly shows that multilayer LB films of the gold nanoparticle monolayer organized at the air-water interface may be grown without a significant change in the cluster density in the different layers.

The monolayer protected gold particles are reported to have a tendency to form large three-dimensional superstructures at room temperature^[122]. This occurs by a process termed digestive ripening which involves refluxing of gold nanoparticles in the presence of an excess of capping ligand. This process transforms polydisperse nanoparticles in solution into highly monodisperse ones, often by a method of ligand exchange^[123].

Optical Properties

For a spherical nanoparticle much smaller than the wavelength of light, an electromagnetic field at a certain frequency induces a resonant, coherent oscillation of metal free electrons across the nanoparticle. This oscillation is known as the surface plasmon resonance (SPR) [Figure 5]^[124]. The resonance lies at visible frequencies for the gold and silver nanoparticles^[124]. The surface Plasmon oscillation of the metal electrons results in a strong enhancement of absorption and scattering of electromagnetic radiation in resonance with the SPR frequency of the noble metal nanoparticles, giving them intensive colors and interesting optical properties^[125].

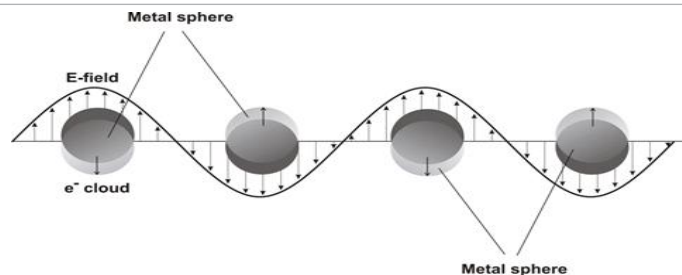


Figure 5. Schematic of the interaction of a metal nanosphere with light^[126].

In general, a colloidal solution of gold nanoparticles (AuNPs) with diameters of 5-20 nm exhibits a red color, because such nanoparticles have an optical absorption peak^[126] around 520 nm caused by surface plasmon resonance^[127]. The optical spectra of AuNP show a localized surface plasmon (LSP) band in the region of 520-550 nm. The interactions of LSP of AuNP and, specifically, of charged AuNP with the surface plasmon excited on the surface of the bulk gold are of special interest and could be studied by the surface plasmon resonance (SPR) technique. The frequency and cross-section of SPR absorption and scattering is dependent on the metal composition, nanoparticle size and shape, dielectric properties of the surrounding medium, and presence of inter-particle interactions^[128]. The extreme sensitivity of the bandwidth, the peak height, and the position of the absorption (or scattering) maximum of SPR spectra to environmental changes has prompted the development of gold nanoparticle-based sensors^[129] including those which directly monitor DNA hybridization^[130].

The surface plasmon resonance and large effective scattering cross section of individual gold nanoparticles make them ideal candidates for molecular labeling, where phenomena such as surface enhance Raman scattering (SERS) can be exploited. UV-visible spectroscopy is a valuable tool for structural characterization of gold nanoparticles. It is well known that the optical absorption spectra of noble metal nanoparticles are dominated by surface plasmon resonances (SPR), which shift to longer wavelengths with increasing particle size^[131]. Also, it is well recognized that the absorbance of gold nanoparticles depends mainly upon size and shape^[132]. In general, the number of SPR peaks decrease as the symmetry of the nanoparticle increases^[133]. Furthermore, gold nanoparticles have exceptionally high absorption coefficients, allowing higher sensitivity in optical detection methods than conventional dyes. The strong absorption of AuNPs has been advantageously used in colorimetric detection of analytes, either by inducing aggregation of AuNPs in the presence of specific analytes, or by measuring changes in the refractive index of the AuNPs environment, due to adsorption of biological analytes. The great enhancement of electromagnetic field at the surface of AuNPs by interaction with electromagnetic radiation offers other interesting optical properties with great potential for bio diagnostic assays^[134].

Gold nanoparticle surfaces can efficiently quench emission from dyes located within a few nanometers of the surface^[135]. Therefore, when fluorophore probes are attached to metallic surfaces, the surface can provide fluorescence quenching, and no organic quencher dye is required. The presence of metals provides alternative nonradiative energy decay paths that can change the fluorescence quantum yield of a fluorophore. At close distances (<5 nm) fluorescence is quenched and at intermediate

distances (7.5–10.0 nm), it is enhanced^[135]. A number of groups have used this phenomenon in a biological assay. Perez-Luna et al^[136] have used a gold surface to quench fluorescence of bound molecules and detected emission after displacement in a competitive immunoassay. Others have attached fluorescently labeled oligonucleotides to gold surfaces, to demonstrate proof of principle for nucleic acid assays.

Fluorescence from the unstructured probes could be quenched because, when oligonucleotides are single stranded, they have flexibility and can form looped structures due to their attraction to the gold surface. In addition, the fluorescent dyes will reversibly absorb onto colloidal gold^[137]. Upon hybridization the double-stranded DNA is rigid such that the fluorescent dye cannot reach the surface. The major shortcoming of both solution based and particle based molecular beacons are the limited multiplexability^[138].

Du et al^[139] demonstrated quenching of hairpin DNA sequences attached to a planar gold surface, to mimic a microarray experiment, and successfully distinguished two DNA sequences, and more recently expanded this work to investigate the thermodynamic and kinetic response of the sensor^[140]. Dubretret et al^[141] used a hairpin loop beacon probe structure on 1.4 nm gold particles, while Maxwell et al^[142] showed that even unstructured oligonucleotide probes could be employed.

It is known that by changing the shape of gold nanoparticles from spheres to elongated rods, the optical characteristics can be significantly changed^[143]. Gold nanorods possess, in addition to an SPR band around 530 nm that corresponds to the transverse Plasmon oscillation, a stronger band at longer wavelengths arising from the Plasmon oscillation of electrons along the longitudinal axis of the nanorods^[144]. The longitudinal Plasmon resonance maximum can be shifted into the near IR region by an increase in the nanorod aspect ratio^[145].

Gold nanoparticles with a diameter 20 nm show essentially only surface Plasmon enhanced absorption with negligible scattering^[146]. However, when the particle diameter is increased from 20 to 80 nm, the relative contribution of surface Plasmon scattering to the total extinction of the particle increases. A colloidal solution of 20 nm AuNPs possesses an intensive ultraviolet-visible light extinction band centered on 520 nm (a deep-red color). This SPR band shifts to higher wavelengths with increasing nanoparticle diameter^[147]. Thus, the color of AuNPs can be tuned by changing their size. The nanoparticle SPR can also be red-shifted by the self-assembly or aggregation of nanoparticles^[148]. The nanoparticle Plasmon resonance shifts to higher wavelengths with increasing refractive index of the medium^[149]. Silver nanoparticles feature is the characteristic absorption at 400–500 nm^[150]. However, the absorption levels obtained in the presence of silver nanoparticles were lower than the ones of the gold nanoparticles.

For multiple assays, however, it is highly desirable to have two markers of different color^[151]. The simplest choice is the exploitation of silver nanoparticles whose LSPR absorption (or scattering) maximum occurs at a wavelength different from that of the gold nanoparticles. Functionalization of silver nanoparticles by different organic ligands has proved to be particularly difficult compared to gold nanoparticles^[152]. Aggregation of the silver or gold nanoparticles shifts the absorption peak toward longer wavelength and changes the color of the final colloidal solution^[42]. The regulated aggregation is used in some

sensing systems.

Mock and coworkers^[153] correlated the absorption spectra of individual silver nanoparticles with their size (40–120 nm) and shape (spheres, decahedrons, triangular truncated pyramids and platelets) determined by TEM. They found that spherical and roughly spherical nanoparticles, decahedral or pentagonal nanoparticles, and triangular truncated pyramids and platelets absorb in the blue, green and red part of the spectrum, respectively. In all the cases the SPR peak wavelength increases with size, as expected.

Fluorescence from the unstructured probes could be quenched because, when oligonucleotides are single stranded, they have flexibility and can form looped structures due to their attraction to the gold surface. In addition, the fluorescent dyes will reversibly absorb onto colloidal silver^[137]. Upon hybridization the double-stranded DNA is rigid such that the fluorescent dye cannot reach the surface. The major shortcoming of both solution-based and particle based molecular beacons are the limited multiplexability^[138].

Gold and Silver Nanoparticle Bio-Conjugates

Metal colloid nanoparticles are known to have both well-defined shapes and controllable size dimensions, being easily available for a variety of metals. Yang et al^[154] have described the fabrication of advanced 1D metallic organic nanocomposites by loading a vacant lipid nanotubes (LNTs) hollow cylinder with water-soluble gold and silver nanoparticles using capillary force [Figure 6]. They achieved the fabrication of gold or silver nanoparticles encapsulated in the cylindrical hollow of the glycolipid nanotube with high-axial ratio by loading the vacant LNT hollow cylinder with aqueous gold or silver nanoparticles using. Aqueous gold or silver nanoparticles (1–3 nm wide) are favorable to form the AuNPs@LNT or AgNPs@LNT nanocomposite in relatively higher yields. This simple and mild approach led to the fabrication of a 1D metallic-organic nanocomposite loading well defined metallic colloid particles inside the organic nanotube hollow. In addition, the 1D nanocomposite functions as a convergent template to fabricate a gold nanowire by removing the LNT shell through a firing process. Thus, the fabrication consists of the following steps: (1) Lyophilization of LNTs to empty the internal hollow volume, (2) filling LNTs with aqueous solution containing metal (Au or Ag) nanoparticles, and (3) removing the LNT shell by firing process. Particle based displays of multiple ligands have the additional advantage of creating a high local concentration of binding molecules. Consequently, binding equilibrium between a surface bound ligand and receptor favors formation of more ligand receptor pairs. For instance, DNA hybridization is thermodynamically favored by 1 order of magnitude if one of the single-stranded (ss) DNA sequences is conjugated to a 10 nm diameter gold nanoparticle surface^[155]. Oligonucleotide derivative nanoparticles have been extensively employed for detecting DNA hybridization in aqueous dispersions and on surfaces^[156]. The overwhelming majority of the use of gold nanoparticles is based on their stability, relative ease of preparation, functionalization, and detection (by absorption or scattering spectroscopy of the intense localized surface plasmon resonance, LSPR). The extreme sensitivity of the bandwidth, the peak height, and the position of the absorption (or scattering) maximum of LSPR spectra to environmental changes has prompted the development of gold nanoparticle-based sensors^[129,130].

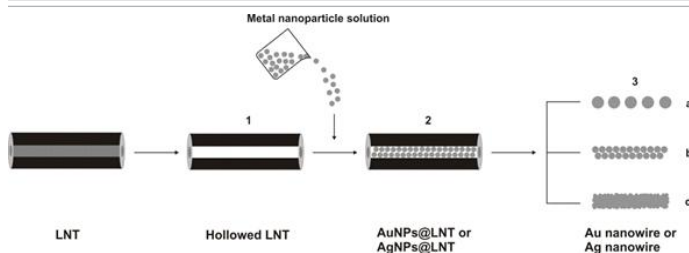


Figure 6. Schematic diagram for the fabrication of AuNPs@LNT or AgNPs@LNT and a gold nanowire. (1) Lyophilization of LNTs to empty the internal hollow volume, (2) filling LNTs with aqueous solution containing metal (Au or Ag) nanoparticles, and (3) removing the LNT shell by firing process: (a) discrete and (b, c) continuous gold nanowires^[154].

Tokareva and Hutter have reported the successful modification of silver and gold nanoparticles by short oligonucleotides of homogeneous sequence, containing only functionalized adenine (A) or thymine (T) (herein referred to as Ag/T, Au/T, Ag/A, and Au/A and hybridized oligonucleotide modified silver and gold nanoparticles as Ag/T-A/Ag, Au/T-A/Au, and Au/T-A/Ag aggregates)^[157]. Authors found that the success of DNA functionalization strongly depends on the sequence of the oligonucleotides. Unlike in the case of gold nanoparticles, A appears to produce more stable silver particles than does T. Analysis of the melting properties of the aggregates in terms of cooperative binding theory points to the lower DNA surface coverage on the Ag/T than that on the Au/T particles. The spectral changes upon hybridization of Ag/T and Ag/A are also strikingly different from those of gold nanoparticles, exhibiting a marked decrease in intensity of the SPR peak, as opposed to a shift of its maximum. This highly different behavior from that of the gold nanoparticles renders silver nanoparticles to be a valuable candidate as a second marker in DNA hybridization experiments. The self-assembly of A and T on gold film and the subsequent hybridization of their complementary pair, unlabeled or labeled by nanoparticles, monitored by Polarization Modulated Fourier Transform Infrared Reflection Absorption Spectroscopy (PM-FTIRAS)^[158], allows us to draw two conclusions. First, the adsorption affinity of oligo (d) A to gold surfaces is high enough to compete with the Au-S bond or the hydrogen bonding to complementary bases; however, the highly loaded Au/T nanoparticles, offering multiple links to the complementary bases, and the attractive force to the gold particle surface are capable of overcoming the nonspecific adsorption of oligo (d) A to the gold film. Second, PM-FTIRAS is not only capable of detecting the base pairing between DNA strands but also it can distinguish between the types of oligonucleotides (adenine or thymine) attached to the nanoparticles.

The fiber surface and the distribution of biotemplated gold on the virus fibers were analyzed using scanning electron microscopy (SEM) and energy dispersive X-ray (EDX) imaging. The homogeneous coating of gold nanoparticles on the genetically functionalized p8#9 fibers indicates the correct presentation of functionalities on the virus fiber surface [Figure 7a]. To demonstrate the specificity of this gold binding ability on genetically engineered M13 virus fibers, fibers were also spun from a wild type clone, M13KE, which does not contain the gold binding functionality. These control fibers contained discrete and scattered gold islands on the fiber surfaces after the identical processing for the p8#9 fibers [Figure. 7b]. Although the surface roughness of virus fibers provides high surface tension,

which may be expected to facilitate nonspecific binding of gold particles onto the fiber, the M13KE fiber itself still exhibited low gold-binding affinity. The low affinity resulted in a low density of gold on the M13KE fiber surface.

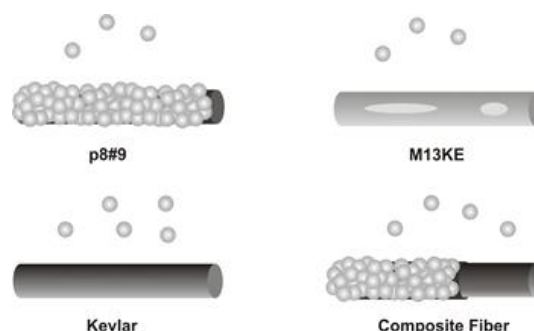


Figure 7. Effects of genetic engineering on mineralization. a) Fiber comprising viruses (p8#9). b) M13KE fiber. c) Kevlar fiber. d) Kevlar fiber coated with p8#9 viruses^[159].

The ability of Kevlar fibers to bind gold was also explored. These synthetic homopolymer fibers showed a negligible amount of gold deposition [Figure. 7c]. Absence of binding affinity to gold and the smooth surface of these synthetic fibers resulted in poor adhesion of gold particles. To create multifunctional fibers having high mechanical strength and capability of surface mineralization, a core @ shell structure was achieved, using Kevlar as the core material and the engineered virus as the shell [Figure 7d].

Both Kevlar and the virus contain functional groups in their chemical structures that contribute to secondary forces, such as hydrogen-bonding and hydrophobic interactions, resulting in adhesion between Kevlar and the virus. After coating with this gold-binding virus, gold nanoparticles were templated directly onto the composite fiber [Figure. 3d]. Although agents such as glutaraldehyde will crosslink the amine groups at the N-termini of pVIII proteins, no disruption of surface functionality of the M13 viruses in these fibers was observed. This demonstrates the capability of the genetically engineered nanometer scale virus scaffold to mineralize inorganic materials at ambient temperature and to retain the desired functionality when assembled as microfibers^[159].

Antimicrobial and Antibacterial Agents

The strong toxicity that some noble metals exhibit in various chemical forms to a wide range of microorganisms is very well known, and, especially, silver nanoparticles have recently been shown to be a promising antimicrobial material. Silver nanoparticles have been studied for their antimicrobial potential and have proven to be antibacterial agents against both Gram-negative and Gram-positive bacteria^[160], and antiviral agents against the HIV-1^[161], Hepatitis B Virus^[162], Respiratory Syncytial Virus^[163], Herpes Simplex Virus type 1^[164] and Monkey Pox Virus^[165].

If we delve into the mechanism of HIV infection, emphasis has been placed on its incomplete elucidation; however, two or three critical steps are implicated:

1. binding of gp120 to the CD4 receptor site on the host cell,
2. induction of a conformational change of gp120, resulting in exposure of new binding sites for a chemokine receptor^[166], and
3. virus entry (to be part of) the cell.

The chemokine receptor, chemokine (C–C motif) receptor 5 (CCR5), probably acts as an essential cofactor for HIV entry and acquisition of infection. Viruses that utilize CCR5 prevail in early stages of mucosal transmission^[167]. This provides an indication that mucosal transmission may selectively involve CCR5, and inevitably emanated in inhibition of CCR5 as a potential microbicide strategy for the prevention of HIV infection. The overall importance of CCR5 for infection across mucosae is thus contentious, as well as the possibility that targeting CCR5 alone may be inadequate to prevent trans-vaginal HIV transmission^[167].

Images obtained by high angle annular dark field (HAADF) and scanning transmission electron microscopy (STEM) show gp120 as its possible molecular target. Using this technique, a regular spatial arrangement of the silver nanoparticles attached to HIV-1 virions was observed. The center-to-center distance between the silver nanoparticles (~28 nm) was similar to the spacing of gp120 spikes over the viral membrane (~22 nm). It was hypothesized that the exposed sulfur-bearing residues of the glycoprotein knobs would be attractive sites for nanoparticle interaction^[166].

By means of a viral adsorption assay, it was shown that silver nanoparticles mechanism of anti-HIV action is based on the inhibition of the initial stages of the HIV-1 cycle. In addition, the gp120-capture ELISA data, combined with the results of the cell-based fusion assay, supported the hypothesis that silver nanoparticles inhibit HIV-1 infection by blocking viral entry, particularly the gp120-CD4 interaction^[168]. The observations made by STEM analysis support this idea, since silver nanoparticles were seen to bind protein structures distributed over the viral membrane^[166]. If silver nanoparticles do not bind to the V3 loop, then they might preferentially interact with the negative cavity of gp120 that binds to CD4^[169]. The attraction between CD4 and gp120 is mostly electrostatic, with the primary end of CD4 binding in a recessed pocket on gp120, making extensive contacts over ~80 nm² of the gp120 surface^[170].

Silver nanoparticles, however, might interact with the two disulfide bonds located in the carboxyl half of the HIV-1 gp120 glycoprotein, an area that has been implicated in binding to the CD4 receptor^[171]. Silver ions bind to sulfhydryl groups, which lead to protein denaturation by the reduction of disulfide bonds^[172]. Therefore, it was hypothesized that silver nanoparticles not only bind to gp120 but also modify this viral protein by denaturing its disulfide-bonded domain located in the CD4 binding region.

High activity of silver nanoparticles was suggested to be due to species difference as they dissolve to release Ag⁰ (atomic) and Ag⁺ (ionic) clusters, whereas silver salts release Ag⁺ only^[173]. The time-of-addition experiments further confirmed silver nanoparticles as entry inhibitors. In addition, it was revealed that silver nanoparticles have other sites of intervention on the viral life cycle, besides fusion or entry. Since silver ions can complex with electron donor groups containing sulfur, oxygen, or nitrogen that are normally present as thiols or phosphates on amino acids and nucleic acids^[174] they might inhibit post-entry stages of infection by blocking HIV-1 proteins other than gp120, or reducing reverse transcription or proviral transcription rates by directly binding to the RNA or DNA molecules. Besides, earlier studies have shown that silver nanoparticles suppress the expression of TNF- α ^[175] which is a cytokine

that plays a pivotal role in HIV-1 pathogenesis by incrementing HIV-1 transcription^[176].

Microbicides are designed to inhibit virus infection by directly inactivating the virus or interrupting its attachment, entry, or replication^[177]. Recent insights into how HIV infiltrates the genital mucosa, initial interactions with immune cells and the role of dendritic cells in transporting the virus to the lymph nodes have suggested numerous potential new targets for microbicides^[178, 179].

Bowman and co-workers^[180] have documented the first application of small-molecule coated gold nanoparticles as effective inhibitors of virus fusion. The gold nanoparticles employed as a platform (2.0 nm diameter) transformed a weakly binding and biologically inactive small molecule into a multivalent conjugate that effectively inhibited HIV-1 fusion to human T-cells. Of significance is the similarity of this class of gold particles to proteins and dendrimers in terms of their atomical precision and mono-disperse nanosize^[180]. The mercapto benzoic acid-coated gold nanoparticles were conjugated to SDC-1721, a derivative of TAK-779, which is a known CCR5 antagonist. Free SDC-1721 had no inhibitory effect on HIV infection; however, the (SDC-1721)-gold nanoparticle conjugate displayed activity comparable to that of TAK-779^[181]. This molecule was thus instituted to demonstrate the feasibility of conjugating a low affinity, biologically inactive small molecule to a gold nanoparticle for the design of biologically active multivalent gold nanoparticle therapeutics. The mechanism of inhibition of viral replication was specific for viral entry^[180]. A significant contribution was thus made by this study in demonstrating the first application of small molecule coated gold nanoparticles as effective inhibitors of HIV fusion. The demonstration that therapeutically inactive monovalent small organic molecules may be converted into highly active drugs by simply conjugating them to gold nanoparticles is considered to add impetus to the discovery of effective new drug formulations^[181].

Conclusion

Noble metal nanomaterials have been synthesized using a variety of methods, including hard template, chemical and bio-reduction and synthesis in micellar solutions (soft templates). Two main approaches can be employed for the preparation of noble metal nanoparticles: coprecipitation (supersaturation) and chemical reduction. In both cases, the presence of surfactant is required to govern the growth process. Generation of supersaturation through in situ chemical reactions by converting highly soluble chemicals into less soluble chemicals starts the formation of primary particles and governs the growth and aggregation events. The chemical reduction occurring in colloidal assemblies is another approach for the formation of size and shape controlled nanoparticles.

The successful utilization of gold and silver nanoparticles (AuNPs and AgNPs) in biological assays relies on the availability of synthetic methods generating nanoparticles with the desired characteristics, namely high solubility in water, and adequate morphology, size dispersion, and surface functionalities. Control over the shape and size of the AuNPs and AgNPs is usually achieved through the careful selection of the experimental conditions, namely reducing agent, reaction time, temperature, and capping agent. An interesting approach might be to use cap-

ping agents with weak and strong affinity for gold and silver, for example, in the mixed precursor systems. This might lead to the different compositions from the core @ shell to alloys.

Of the chemical processes, reverse micelle (microemulsion (soft template)) synthesis has been recently demonstrated to be a viable method for producing a wide array of metal and metal oxide nanoparticles over a relatively narrow particle size distribution. Micelle formation allows for a unique encapsulated volume of controllable size through which reactions and subsequent development of metal and metallic compounds can be produced. The co-surfactants and various additives are known to influence the micelle size and shape and therefore might also regulate the size and the form of final metal nanoparticles.

The ligand exchange reaction is an extremely versatile tool for the preparation of functionalized metal nanoparticles. This method is fast and simple to use; it allows one to introduce functional groups that are incompatible with other methods for nanoparticle synthesis. The strong interaction between n-alkylthiols and the gold surface provides the most popular method for the attachment of molecular groups. Precise, angstrom-level control of reactivity in nanotechnology requires nanoscale building blocks of known structure at atomic resolution. Functionalization of gold and silver nanoparticles involves the use of functional ligands in which a moiety is used for anchorage to the particle while the other is directed to the outer surface for specific interaction with biomolecules. Functionalization of AuNPs with biomolecules has also been used in order to develop methodologies suitable for clinical diagnostics. To apply gold colloids in newly developed bio modifying medical assay systems, a simple and facile means of anchoring different ligand biomolecules onto particle surfaces are strongly required as well as the stability in the physiological condition should be improved. Colloidal gold nanoparticles, in particular, have found application in a variety of assay formats in which analyte binding is coupled to particle adsorption.

The unique physical properties of nanoscale noble metal gold materials have generated considerable interest for their use in a wide range of diverse applications from data information storage to in vivo optical and magnetic manipulation in biomedical systems. Nanoparticles exhibit novel material properties which largely differ from the bulk materials due to these small sizes, including quantum size effect on photochemistry, nonlinear optical properties of semiconductor or the emergence of metallic properties with the size of the particles. As nanomaterials of gold nanoparticles have extensive applications, such as composites based on interaction of gold nanomaterials with DNA, viruses, proteins, antibacterial materials, antistatic materials, cryogenic superconducting materials, biosensor materials and so on. The surface plasmon resonance and large effective scattering cross section of individual gold nanoparticles make them ideal candidates for molecular labeling, where phenomena such as surface enhance Raman scattering (SERS) can be exploited. It is well known that the optical absorption spectra of noble metal nanoparticles are dominated by surface plasmon resonances (SPR), which shift to longer wavelengths with increasing particle size. Also, it is well recognized that the absorbance of gold nanoparticles depends mainly upon size and shape. The extreme sensitivity of the bandwidth, the peak height, and the position of the absorption (or scattering) maximum of SPR spectra to environmental changes has prompted the development of

gold nanoparticle-based sensors including those which directly monitor DNA hybridization.

The noble metal nanoparticles are known to exhibit various chemical forms with some microorganisms and, especially, silver nanoparticles have recently been shown to be a promising antimicrobial material. They form very interesting smart nanobioconjugates and nanostructures functioning as biosensors. Silver nanoparticles have been studied for their antimicrobial potential and have proven to be antibacterial agents against both Gram-negative and Gram-positive bacteria, and antiviral agents against the HIV-1, Hepatitis B virus, Respiratory Syncytial Virus, Herpes Simplex Virus type 1 and Monkey Pox Virus. We speculate that the alloys of noble metal nanoparticles could be interesting for the interactions with various microorganisms that is, with their DNA and peptides. The small amount of silver is known to strongly influence the plasmon band intensity and position. The similar behavior might be found for alloy nanoparticles against the various bacteria and viruses.

Acknowledgement

This research is supported by the VEGA grants 2/0040/14 and 2/0152/13 and APVV-0125-11.

Abbreviations

A: Adenine; AFM: Atomic Force Microscopy; AgNP: Silver Nanoparticle; AOT: sodiumbis(2-thylhexyl) sulfosuccinate ; AuNP : Gold Nanoparticle; DDAB: Dido decyldimethyl ammonium Bromide; DLS: Dynamic Light Scattering; DLVO Theory: Derjaguin Landau Verwey Overbeek Theory; DNA: Deoxyribonucleic Acid; EDX: Energy Dispersive X-Ray; ELISA: Enzyme Linked Immunosorbent Assay; GP: Glycoprotein; HAADF: High Angle Annular Dark Field; HIV: Human Immuno Deficiency Virus; LB Film: Langmuir-Blodgett Film; LNTs: Lipid Nanotubes; LSP Localized Surface Plasmon; MPCs: Monolayer Protected Clusters; NCS: Nanocrystal Superlattice; NPs: Nanoparticles; [Pd(oct-en)₂]Cl₂ bis(N-octylethylenediamine): Palladium (II) Chloride; PM-FTIRRAS: Polarization Modulated Fourier Transform Infrared Reflection Absorption Spectroscopy; PVP: Polyvinyl pyrrolidone; QCM: Quartz Crystal Microbalance; RSH: Alkylthiol; RSSR: Dialkyldisulfide; SAM: Self-Assembled Monolayer SEM: Scanning Electron Microscopy; SERS: Surface Enhance Raman Scattering; SPR: Surface Plasmon Resonances; STEM: Scanning Transmission Electron Microscopy; T: Thymine; TEM: Transmission Electron Microscopy; TPP: Triphenylphosphine

References

1. Service, R. F. Small clusters hit the big time. (1996) *Science* 271: 920-922.
2. Sun, S., Murray, C. B., Weller, D., et al. Monodisperse FePt nanoparticles and ferromagnetic FePt nanocrystal superlattices. (2000) *Science* 287(5460): 1989-1992.
3. Feldmann, C. Polyol-Mediated Synthesis of Nanoscale Functional Materials. (2003) *Adv Funct Mater* 13(2): 101-107.
4. Jiang, H. Q., Manolache, S., Wong, A. C. L., et al. Plasma-enhanced Deposition of Silver Nanoparticles onto Polymer and Metal Surfaces for the Generation of Antimicrobial Characteristics. (2004) *J Appl Polym Sci* 93(3): 1411-1422.

5. Hirano, S., Wakasa, Y., Saka, A., et al. Preparation of Bi-2223 bulk composed with silver-alloy wire. (2003) *Phys C* 392: 458-462.
6. Modi, A., Koratkar, N., Lass, E., et al. Miniaturized gas ionization sensors using carbon nanotubes, (2003) *Nature* 424(6945): 171-174.
7. Brust, M., Walker, M., Bethell, D., et al. Synthesis of thiol-derivatized gold nanoparticles in a two-phase Liquid-Liquid system. (1994) *J Chem Soc Chem Commun* (7): 801-802.
8. Shon, Y. S., Mazzitelli, C., Murray, R. W. Unsymmetrical disulfides and thiol mixtures produce different mixed monolayer-protected gold clusters. (2001) *Langmuir* 17(25): 7735-7741.
9. Li, X. M., de Jong, M. R., Inoue, K. S., et al. Formation of gold colloids using thioether derivatives as stabilizing ligands. (2001) *J Mater Chem* 11(7): 1919-1923.
10. Boal, A. K., Ilhan, F., DeRouchey, J. E., et al. Self-assembly of nanoparticles into structured spherical and network aggregates. (2002) *Nature* 404(6779): 746-748.
11. Brousseau, L. C., Novak, J. P., Marinakos, S. M et al. Assembly of Phenylacetylene-Bridged Gold nanocluster Dimers and Trimers. (1999) *Adv. Mater* 11: 447-449.
12. Maye, M. M., Chun, S. C., Han, L., et al. Novel Spherical Assembly of Nanoparticles Mediated by a Thioether. (2002) *J Am Chem Soc* 124: 4958-4959.
13. Li, Y., Leung, P., Yao, L., et al. Antimicrobial effect of surgical masks coated with nanoparticles. (2006) *J Hosp Infect* 62(1): 58-63.
14. Bhattacharya, R., Mukherjee, P. Biological properties of "naked" metal nanoparticles. (2008) *Adv Drug Deliv Rev* 60(11): 1289-1306.
15. Siegel, R. W., Ramasamy, S., Hahn, H., et al. Synthesis, characterization, and properties of nanophase TiO₂. (1988) *J Mater Res* 3(6): 1367-1372.
16. Fegley, B. J., White, P., Bowen, H. K., et al. Processing and Characterization of ZrO₂ and Y-doped ZrO₂ Powders. (1985) *Am Ceram Soc Bull* 64(8): 1115-1120.
17. Fayet, P., Woste, L. Experiments on Size-Selected Metal Cluster Ions in a Triple Quadrupole Arrangement. (1986) *Zeitschrift für Physik D Atoms Molecules and Clusters* 3(2): 177-182.
18. Tang, Z. X., Sorensen, C. M., Klabunde, K. J., et al. Preparation of Manganese Ferrite Fine Particles from Aqueous Solution. (1991) *J Colloid Interface Sci* 146(1): 38-52.
19. Dumestre, F., Chaudret, B., Amiens, C., et al. Shape control of thermodynamically stable cobalt nanorods through organometallic chemistry. (2002) *Angew Chem* 41(22): 4286-4289.
20. Pileni, M. P. Role of soft colloidal templates in the control of size and shape of inorganic nanocrystals. (2003) *Nat Mater* 2(3): 145-150.
21. Jana, N. R., Gearheart, L., Murphy, C. J. Wet chemical synthesis of high aspect ratio cylindrical gold nanorods. (2001) *Journal of Physical Chemistry B* 105(19): 4065-4067.
22. Green, M. Organometallic based strategies for metal nanocrystal synthesis. (2005) *Chem Commun*. 24: 3002-3011.
23. Turkevich, J., Stevenson, P. C., Hillier, J. A study of the nucleation and growth processes in the synthesis of colloidal gold. (1951) *Discuss Faraday Soc* 11: 55-75.
24. Hyeon, T., Lee, S. S., Park, J., et al. Synthesis of Highly Crystalline and Monodisperse Magnetite Nanocrystallites without a Size-Selection Process. (2001) *J Am Chem Soc* 123(51): 12798-12801.
25. Glomm, W. R. J. Gold Nanoparticles for Applications in Bionanotechnology. (2005) *Dispersion Sci Technol* 26(3): 389-414.
26. Hunter, R. J. *Foundations of Colloid Science*; Oxford University Press: New York (2001).
27. Hiramatsu, H., Osterloh, F. E. A Simple Large Scale Synthesis of Nearly Monodisperse Gold and Silver Nanoparticles with Adjustable Sizes and with Exchangeable Surfactants. (2004) *Chem Mater* 16(13): 2509-2511.
28. Jana, N. R., Peng, X. G. Single-phase and gram-scale routes toward nearly monodisperse Au and other noble metal nanocrystals. (2003) *J Am Chem Soc* 125(47): 14280-14281.
29. Capek, I. *Nanocomposite structures and dispersions*, Eds D Mobius and R Muller. (2006) Elsevier London.
30. Misra, R. D. K., Gubbala, S., Kale, A., et al. A comparison of the magnetic characteristics of nanocrystalline nickel, zinc, and manganese ferrites synthesized by reverse micelle technique. (2004) *J Mater Sci Eng B* 111: 164-174.
31. McLeod, M. C., McHenry, R. S., Beckman, E. J. Synthesis and stabilization of silver metallic nanoparticles and premetallic intermediates in perfluoropolyether/CO₂ reverse micelle systems. (2003) *J Phys Chem B* 107(12): 2693-2700.
32. Jain, T. K., Cassin, G., Badiali, J. P., et al. Relation between Exchange Process and Structure of AOT Reverse Micellar System. (1996) *Langmuir* 12(10): 2408-2411.
33. Capek, I. Preparation of metal nanoparticles in water-in-oil (w/o) microemulsions *Adv. Colloid Interface*. (2004) *Sci* 110(1-2): 49-74.
34. Murphy, C. J., Jana, N. R. Controlling the Aspect Ratio of Inorganic Nanorods and Nanowires. (2002) *Adv Mater* 14: 80-82.
35. Roucoux, A., Schultz, J. Reduced transition metal colloids: A novel family of reusable catalysts? (2002) *H Patin Chem Rev* 102(10): 3757-3778.
36. Jana, N. R. Shape Effect in Nanoparticle Self-Assembly. (2004) *Angew Chem* 43(12): 1536-1540.
37. Jana, N. R., Pal, T. Acid-Base Equilibria in Aqueous Micellar Medium: A Comprehensive Review. (2001) *J Surf Sci Technol* 17: 191-212.
38. Toernblom, M., Henriksson, U. Effect of solubilization of aliphatic hydrocarbons on size and shape of rodlike C16 TABr micelles studied by 2H NMR relaxation. (1997) *J Phys Chem B* 101(31): 6028-6035.
39. Lin, Z., Cai, J. J., Scriven, L. E., et al. Spherical-to-Wormlike Micelle Transition in CTAB Solutions. (1994) *J Phys Chem* 98(23): 5984-5993.
40. Lin, X. M., Sorensen, C. M., Klabunde, K. J. Digestive ripening, nanophase segregation and superlattice formation in gold nanocrystal colloids. (2000) *J Nanoparticle Res* 2: 157-164.
41. Dubbois, L. H., Nuzzo, R. G. Synthesis, Structure, and Properties of Model Organic Surfaces. (1992) *Annu Rev Phys Chem* 43: 437-463.
42. Krebig, U., Genzel, L. Optical absorption of small metallic particles. (1985) *Surface Sci* 156(2): 678-700.
43. Djalali, R., Chen, Y. F., Matsui, H. Au nanocrystal growth on nanotubes controlled by conformations and charges of sequenced peptide templates. (2003) *J Am Chem Soc* 125(19): 5873-5879.
44. Keren, K., Berman, R. S., Buschstab, E., et al. DNA-templated carbon nanotube field-effect transistor. (2003) *Science* 302(5649): 1380-1382.
45. Djalali, R., Samson, J., Matsui, H. Doughnut-shaped peptide nano-assemblies and their applications as nanoreactors. (2004) *J Am Chem Soc* 126(25): 7935-7939.
46. Matsui, H., Gologan, B. Crystalline Glycylglycine Bolaamphiphile Tubules and Their pH-Sensitive Structural Transformation. (2000) *J Phys Chem B* 104(15): 3383-3386.
47. Manna, A., Imae, T., Aoi, K., et al. Synthesis of dendrimer-passivated noble metal nanoparticles in a polar medium: Comparison of size between silver and gold particles. (2001) *Chem Mater* 13(5): 1674-1681.
48. Worden, J. G., Shaffer, A. W., Huo, Q. Controlled functionalization of gold nanoparticles through a solid phase synthesis approach. (2004) *Chem Commun* (5): 518-519.
49. Sung, K. M., Mosley, D.W., Peelle, B. R., et al. Synthesis of monofunctionalized gold nanoparticles by fmoc solid-phase reactions. (2004) *J Am Chem Soc* 126(16): 5064-5065.
50. Zhang, W., Qiao, X., Chen, J. Synthesis of nanosilver colloidal particles in water/oil microemulsion. (2007) *Colloids and Surfaces A: Physicochem Eng Aspects* 299(1-3): 22-28.
51. Zhang, W. Z., Qiao, X. L., Chen, J. G., et al. Preparation of silver nanoparticles in water-in-oil AOT reverse micelles. (2006) *J Colloid Interface Sci* 302(1): 370-373.
52. He, B. L., Tan, J. J., Kong, Y. L., et al. Synthesis of size controlled Ag nanoparticles. (2004) *J Mol Catal A Chem* 221(1-2): 121-126.
53. Ahmadi, T. S., Wang, Z. L., Green, T. C., et al. Shape-Controlled Synthesis of Colloidal Platinum Nanoparticles. (1996) *Science* 272(5270): 1924-1926.

54. Fu, X., Wang, Y., Wu, N., et al. Shape-selective preparation and properties of oxalate-stabilized Pt colloid. (2002) *Langmuir* 18(12): 4619-4624.
55. Chen, J., Herricks, T., Geissler, M., et al. Single-crystal nanowires of platinum can be synthesized by controlling the reaction rate of a polyol process. (2004) *J Am Chem Soc* 126(35): 10854-10855.
56. Herricks, T., Chen, J., Xia, Y. Polyol Synthesis of Platinum Nanoparticles: Control of Morphology with Sodium Nitrate. (2004) *Nano Lett* 4(12): 2367-2371.
57. Yu, Y., Xu, B. Selective formation of tetrahedral Pt nanocrystals from K₂PtCl₆/PVP. (2003) *Chin Sci Bull* 48(23): 2589-2593.
58. Narayanan, R., El-Sayed, M. A. Effect of Colloidal Nanocatalysis on the Metallic Nanoparticle Shape: The Suzuki Reaction. (2005) *Langmuir* 21(5): 2027-2033.
59. Narayanan, R., El-Sayed, M. A. Effect of nanocatalysis in colloidal solution on the tetrahedral and cubic nanoparticle shape: Electron-transfer reaction catalyzed by platinum nanoparticles. (2004) *J Phys Chem B* 108(18): 5726-5733.
60. Narayanan, R., El-Sayed, M. A. Shape-Dependent Catalytic Activity of Platinum Nanoparticles in Colloidal Solution. (2004) *Nano Lett* 4(7): 1343-1348.
61. Narayanan, R., El-Sayed, M. A. Changing catalytic activity during colloidal platinum nanocatalysis due to shape changes: Electron-transfer reaction. (2004) *J Am Chem Soc* 126(23): 7194-7195.
62. Narayanan, R., El-Sayed, M. A. Effect of Catalytic Activity on the Size Distribution of Metallic Nanoparticles: Electron Transfer Reaction Between Fe(CN)₆-3 and Thiosulfate Ions Catalyzed by PVP-Platinum Nanoparticles. (2003) *J Phys Chem B* 107(45): 12416-12424.
63. Narayanan, R., El-Sayed, M. A. Catalysis with transition metal nanoparticles in colloidal solution: Nanoparticle shape dependence and stability. (2005) *J Phys Chem B* 109(26): 12663-12676.
64. Ingelsten, H. H., Bagwe, R., Palmqvist, A., et al. Kinetics of the Formation of Nano-Sized Platinum Particles in Water-in-Oil Microemulsions. (2001) *J Colloid Interface Sci* 241(1): 104-111.
65. Fletcher, P. D. I., Howe, A. M., Robinson, B. H. The kinetics of solubilisation exchange between water droplets of a water-in-oil microemulsion. (1987) *J Chem Soc Faraday Trans 1*(83): 985-1006.
66. Shelimov, B. N., Lambert, J. F., Che, M., et al. Molecular-level studies of transition metal-support interactions during the first steps of catalysts preparation: platinum speciation in the hexachloroplatinate/alumina system. (2000) *J Mol Catal A* 158(1): 91-99.
67. Rivadulla, J. F., Vergara, M. C., Blanco, M. C., et al. Optical Properties of Platinum Particles Synthesized in Microemulsions. (1997) *J Phys Chem B* 101(44): 8997-9004.
68. Creighton, A., Eadon, D. Ultraviolet-visible absorption spectra of the colloidal metallic elements. (1991) *J Chem Soc Faraday Trans 87*: 3881-3891.
69. Barnickel, P., Wokaun, A., Sager, W., et al. Size tailoring of silver colloids by reduction in w/o microemulsions. (1992) *J Colloid Interface Sci* 148(1): 80-90.
70. Sheu, E. Y., Chen, S. H. Thermodynamic Analysis of Polydispersity in Ionic Micellar Systems and Its Effect on SANS Data Treatment. (1988) *J Phys Chem* 92(15): 4466-4474.
71. Zhang, X., Chan, K. Y. Water-in-Oil Microemulsion Synthesis of Platinum-Ruthenium Nanoparticles, Their Characterization and Electrocatalytic Properties. (2003) *Chem Mater* 15(2): 451-459.
72. Chen, D. H., Wu, S. H. Synthesis of nickel nanoparticles in water-in-oil microemulsions. (2000) *Chem Mater* 12(5): 1354-1360.
73. Iida, M., Ohkawa, S., Er, H., et al. Formation of Palladium(0) Nanoparticles from a Microemulsion System Composed of Bis (N-octylethylenediamine)palladium(II) Chloride Complex. (2002) *Chem Lett* 10: 1050-1051.
74. Hamada, K., Hatanaka, K., Kawai, T., et al. On palladium nanoparticles formation by reverse microemulsion of bis(N-octylethylenediamine)palladium(II) chloride. (2000) *Shikizai Kyokaishi* 73: 385-392.
75. Ostwald, W. Studies on the formation and transformation of solid bodies. (1897) *Journal of physical Chemistry* 22: 289-330.
76. Smet, Y. De., Deriemaeker, L., Finsy, R. A simple computer simulation of Ostwald ripening. (1997) *Langmuir* 13(26): 6884-6888.
77. Ostwald, W. About the supposed isomerism of red and yellow mercuric oxide and the upper flashing voltage-proof body. (1900) *Z Phys Chem* 34: 495-503.
78. Lin, X. M., Wang, G. M., Sorensen, C. M., et al. Formation and dissolution of gold nanocrystal superlattices in a colloidal solution. (1999) *J Phys Chem B* 103: 5488-5492.
79. Stoeva, S., Klabunde, K. J., Sorensen, C. M., et al. Gram Scale Synthesis of Monodisperse Gold Colloids by the Solvated Metal Atom Dispersion (SMAD) Method and their Organization into two- and three-dimensional Structures. (2002) *J Am Chem Soc* 124(10): 2305-2311.
80. Ferrell, T. L., Callcott, T. A., Warmark, R. Plasmons and surfaces. (1985) *J Am Sci* 73: 344-353.
81. Lin, S. T., Franklin, M. T., Klabunde, K. J. Nonaqueous colloidal gold. Clustering of metal atoms in organic media-12. (1986) *Langmuir* 2(2): 259-260.
82. Klabunde, K. J., Mulukutla, R. S. *Nanoscale Materials in Chemistry*. Klabunde, K. J., Wiley, Ed. (2001) Interscience New York Chapt 7: 223-261.
83. Hostetler, M. J., Templeton, A. C., Murray, R.W. Dynamics of place-exchange reactions on monolayer-protected gold cluster molecules. (1999) *Langmuir* 15: 3782-3789.
84. Song, Y., Huang, T., Murray, R. W. Heterophase Ligand Exchange and Metal Transfer between Monolayer Protected Clusters. (2003) *J Am Chem Soc* 125(38): 11694-11701.
85. Schmid, G., Pfeil, R., Boese, R., et al. Au₃₅P(C₆H₅)₃.12C₁₆ – a gold cluster of unusual size. (1981) *Chem Ber* 114(11): 3634-3642.
86. Warner, M. G., Reed, S. M., Hutchison, J. E. Small, Water-soluble, Ligand-stabilized Gold Nanoparticles Synthesized by Interfacial Ligand Exchange Reactions. (2000) *Chem Mater* 12(11): 3316-3320.
87. Storhoff, J. J., Elghanian, R., Mucic, R. C., et al. One-Pot Colorimetric Differentiation of Polynucleotides with Single Base Imperfections Using Gold Nanoparticle Probes. (1998) *J Am Chem Soc* 120: 1959-1964.
88. Templeton, A. C., Wuelfing, W. P., Murray, R. W. Monolayer-protected cluster molecules. (2000) *Acc Chem Res* 33(1): 27-36.
89. Houseman, B. T., Mrksich, M. The Role of Ligand Density in the Enzymatic Glycosylation of Carbohydrates Presented on Self-Assembled Monolayers of Alkanethiolates on Gold. (1999) *Angew Chem Int Ed* 38(6): 782-785.
90. Bain, C. D., Evall, J., Whitesides, G. M. Formation of Monolayers by the Coadsorption of Thiols on Gold: Variation in the Head Group, Tail Group, and Solvent. (1989) *J Am Chem Soc* 111: 7155-7164.
91. Feldheim, D. L., Keating, C. D. Self-assembly of single electron transistors and related devices. (1998) *Chem Soc Rev* 27: 1-12.
92. Hsieh, B. Y., Chang, Y. F., Ng, M. Y., et al. Localized surface plasmon coupled fluorescence fiber-optic biosensor with gold nanoparticles. (2007) *Anal Chem* 79(9): 3487-3493.
93. Ojeda, R., de Paz, J. L., Barrientos, A. G., et al. Preparation of multifunctional glyconanoparticles as a platform for potential carbohydrate based anticancer vaccines. (2007) *Carbohydr Res* 342(3-4): 448-459.
94. You, C. C., Verma, A., Rotello, V. M. Engineering the nanoparticle-biomacromolecule interface. (2006) *Soft Matter* 2: 190-204.
95. Levy, R. Peptide Capped Gold Nanoparticles: Towards Artificial Proteins. (2006) *Chembiochem* 7(8): 1141-1145.
96. Giersig, M., Mulvaney, P. Preparation of ordered colloid monolayers by electrophoretic deposition. (1993) *Langmuir* 9(12): 3408-3413.
97. Cleveland, C. L., Landman, U., Shafiqullin, M. N., et al. Structural Evolution of Larger Gold Clusters. (1997) *Z Phys D* 40: 503-508.
98. Lin, X. M., Sorensen, C. M., Klabunde, K. J. Ligand-Induced Gold Nanocrystal Superlattice Formation in Colloidal Solution. (1999) *Chem Mater* 11(2): 198-202.
99. Lin, X. M., Jaeger, H.M., Sorensen, C. M., et al. Formation of Long-Range-Ordered Nanocrystal Superlattices on Silicon Nitride Substrates. (2001) *J Phys Chem B* 105: 3353-3357.
100. Korgel, B. A., Fitzmaurice, D. Condensation of Ordered Nano-

- crystal Thin Films. (1998) *Phys Rev Lett* 80: 3531-3534.
101. Deegan, R. D., Bakajin, O., Dupont, T. F., et al. Capillary flow as the cause of ring stains from dried liquid drops. (1997) *Nature* 389: 827-829.
 102. Ge, G., Brus, L. Evidence for Spinodal Phase Separation in Two-Dimensional Nanocrystal Self-Assembly. (2000) *J Phys Chem B* 104(41): 9573-9575.
 103. Asher, S. A., Holtz, J., Liu, L., et al. Self Assembly Motif for Creating Submicron Periodic Materials. Polymerized Crystalline Colloidal Arrays. (1994) *Am Chem Soc* 116(16): 4997-4998.
 104. Hunter, R. J. Introduction to Modern Colloid Science. (1993) Oxford University Press New York 99(3): 591-592.
 105. Derjaguin, B. V., Landau, L. A theory of the stability of strongly charged lyophobic soils and of the adhesion of strongly charged particles in solution of electrolyte. (1941) *Acta Physicochim USSR* 14: 633-662.
 106. Verwey, E.J.W., Overbeek, J.Th.G. Theory of Stability of Lyophobic Colloids. (1948) Elsevier: Amsterdam.
 107. Israelachvili, J. N. Intermolecular and Surface Forces. (1992) Academic Press: San Diego 246.
 108. Weller, H. Self-Organized Superlattices of Nanoparticles. (1996) *Angew Chem Int Ed Engl* 35(10): 1079- 1081.
 109. Luedtke, W. D., Landman, U. Structure, dynamics, and thermodynamics of passivated gold nanocrystallites and their assemblies. (1996) *J Phys Chem* 100(32): 13323- 13329.
 110. Nuzzo, R. G., Zegarski, B. R., Dubois, L. H. Fundamental studies of the chemisorption of organosulfur compounds on Au(111). Implications for molecular self-assembly on gold surfaces. (1987) *J Am Chem Soc* 109(3): 733-740.
 111. Bain, C. D., Troughton, E. B., Tao, Y. T., et al. Formation of Monolayer Films by the Spontaneous Assembly of Organic Thiols from Solution onto Gold. (1989) *J Am Chem Soc* 111(1): 321-335.
 112. Fenter, P., Eberhardt, A., Eisenberger, P. Self-assembly of n-alkyl thiols as disulfides on Au (111). (1994) *Science* 266(5188): 1216-1218.
 113. Brust, M., Bethell, D., Schiffrin, D.J., et al. Novel gold-dithiol nano-networks with non-metallic electronic properties. (1995) *Adv Mater* 7(9): 795-797.
 114. Storhoff, J. J., Mirkin, C. A. Programmed Materials Synthesis with DNA. (1999) *Chem Rev* 99(7): 1849-1862.
 115. Swami, A., Kumar, A., Selvakannan, P., et al. Langmuir-Blodgett films of laurylamine-modified hydrophobic gold nanoparticles organized at the air-water interface. (2003) *J Colloid Interface Sci* 260(2): 367- 373.
 116. Fendler, J. H., Meldum, F. The colloid chemical approach to nanostructured materials. (1995) *Adv Mater* 7(7): 607- 632.
 117. Bourgoin, J.P., Kergueris, C., Lefevre, E., et al. Langmuir-Blodgett films of thiol-capped goldnanoclusters: fabrication and electrical properties. (1998) *Thin Solid Films* 327-329: 515-519.
 118. Sastry, M., Patil, V., Mayya, K.S., et al. Organization of polymer-capped platinum colloidal particles at the air-water interface. (1998) *Thin Solid Films* 324(1-2): 239- 244.
 119. Bhushan, B., Kulkarni, A.V., Koinkar, V. N., et al. Microtribological Characterization of Self-Assembled and Langmuir-Blodgett Monolayers by Atomic and Friction Force Microscopy. (1995) *Langmuir* 11(8): 3189-3198.
 120. Heath, J.R., Knobler, C.M., Leff, D.V. Pressure/temperature phase diagrams and superlattices of organically functionalized metal nanocrystal monolayers: The influence of particle size, size distribution and surface passivant. (1997) *J Phys Chem B* 101(2): 189- 197.
 121. Sastry, M., Kumar, A., Mukherjee, P. Phase transfer of aqueous colloidal gold particles into organic solutions containing fatty amine molecules. (2001) *Colloids Surf A* 181(1-3): 255-259.
 122. Prasad, B. L. V., Stoeva, S. I., Sorensen, C. M., et al. Digestive Ripened Thiolated Gold Nanoparticles: The Effect of Alkyl Chain Length. (2002) *Langmuir* 18(20): 7515- 7520.
 123. Brown, L.O., Hutchison, J.E. Formation and Electron Diffraction Studies of Ordered 2-D and 3-D Superlattices of Amine-stabilized Gold Nanoparticles. (2001) *J Phys Chem B* 105(37): 8911- 8916.
 124. Link, S., El-Sayed, M. A. Optical properties and ultrafast dynamics of metallic nanocrystals. (2003) *Annu Rev Phys Chem* 54: 331-366.
 125. Mulvaney, P. Surface Plasmon Spectroscopy of Nanosized Metal Particles. (1996) *Langmuir* 12(3): 788-800.
 126. Jain, P.K., El-Sayed, I.H., El-Sayed, M.A. Au nanoparticles target cancer. (2007) *Nano Today* 2(1): 18- 29.
 127. Bohren, C.F., Huffman, D.R. Absorption and Scattering of Light by Small Particles. (1983) John Wiley & Sons: New York.
 128. Jain, P.K., Eustis, S., El-Sayed, M. A. Plasmon Coupling in Nanorod Assemblies: Optical Absorption, Discrete Dipole Approximation Simulation, and Exciton-Coupling Model. (2006) *J Phys Chem B* 110(37): 18243-18253.
 129. Thanh, N.T. K., Rosenzweig, Z. Development of an aggregation-based immunoassay for anti-protein A using gold nanoparticles. (2002) *Anal Chem* 74(7): 1624-628.
 130. Reynolds, R.A., Mirkin, C.A., Letsinger, R.L. A gold nanoparticle/latex microsphere based colorimetric oligonucleotide detection method. (2000) *Pure Appl Chem* 72(1-2): 229-235.
 131. Brause, R., Moeltgen, H., Kleinermanns, K. Characterization of laser-ablated and chemically reduced silver colloids in aqueous solution by UV/VIS spectroscopy and STM/SEM microscopy. (2002) *Applied Physics B: Lasers and Optics* 75: 711-716.
 132. Kerker, M. The optics of colloidal silver: something old and something new. (1985) *Journal of Colloid and Interface Science* 105(2): 297- 314.
 133. Sosa, I. O., Noguez, C., Barrera, R.G. Optical properties of metal nanoparticles with arbitrary shapes. (2003) *Journal of Physical Chemistry B* 107(26): 6269-6275.
 134. Baptista, P., Pereira, E., Eaton, P., et al. Gold nanoparticles for the development of clinical diagnosis methods. (2008) *Anal Bioanal Chem* 391(3): 943-950.
 135. Lakowicz, J. R. Radiative decay engineering: biophysical and biomedical applications. (2001) *Anal Biochem* 298(1): 1-24.
 136. Perez-Luna, V.H., Yang, S., Rabinovich, E.M., et al. Fluorescence biosensing strategy based on energy transfer between fluorescently labeled receptors and a metallic surface. (2002) *Biosens Bioelectron* 17(1-2): 71-78.
 137. Nie, S., Emory, S. R. Probing Single Molecules and Single Nanoparticles by Surface-Enhanced Raman Scattering. (1997) *Science* 275(5303): 1102-1106.
 138. Varma-Basil, M., El-Hajj, H., Marras, S.A., et al. Molecular beacons for multiplex detection of four bacterial bioterrorism agents. (2004) *Clin Chem* 50(6): 1060-1062.
 139. Du, H., Disney, M., Miller, B., et al. Hybridization-based unquenching of DNA hairpins on au surfaces: prototypical "molecular beacon" biosensors. (2003) *J Am Chem Soc* 125(14): 4012- 4013.
 140. Du, H., Strohsahl, C. M., Camera, J., et al. Sensitivity and specificity of metal surface-immobilized "molecularbeacon" biosensors. (2005) *J Am Chem Soc* 127(21): 7932-7940.
 141. Dubertret, B., Calame, M., Libchaber, A. J. Single-mismatch detection using gold-quenched fluorescent oligonucleotides. (2001) *Nat Biotechnol* 19(4): 365-370.
 142. Maxwell, D. J., Taylor, J. R., Nie, S. Self-assembled nanoparticle probes for recognition and detection of biomolecules. (2002) *J Am Chem Soc* 124(32): 9606-9612.
 143. Link, S., El-Sayed, M. A. Simulation of the Optical Absorption Spectra of Gold Nanorods as a Function of Their Aspect Ratio and the Effect of the Medium Dielectric Constant. (2005) *J Phys Chem B* 109(20): 10531-10532.
 144. Link, S., Mohamed, M. B., El-Sayed, M. A. Simulation of the Optical Absorption Spectra of Gold Nanorods as a Function of Their Aspect Ratio and the Effect of the Medium Dielectric Constant. (1999) *J Phys Chem B* 103(16): 3073-3077.
 145. Huang, X., El-Sayed, I.H., Qian, W., et al. Cancer Cell Imaging and Photothermal Therapy in the Near-Infrared Region by Using Gold Nanorods. (2006) *J Am Chem Soc* 128(6): 2115-2120.

146. Jain, P.K., Lee, K.S., El-Sayed, I.H., et al. Calculated absorption and scattering properties of gold nanoparticles of different size, shape, and composition: applications in biological imaging and biomedicine. (2006) *J Phys Chem B* 110(14): 7238-7248.
147. Link, S., El-Sayed, M. A. Size and Temperature Dependence of the Plasmon Absorption of Colloidal Gold Nanoparticles. (1999) *J Phys Chem B* 103(21): 4212-4217.
148. Sonnichsen, C., Reinhard, B.M., Liphardt, J. A molecular ruler based on plasmon coupling of single gold and silver nanoparticles. (2005) *Nat Biotechnol* 23(6): 741-745.
149. Lee, K. S., El-Sayed, M. A. Gold and silver nanoparticles in sensing and imaging: sensitivity of plasmon response to size, shape, and metal composition. (2006) *J Phys Chem B* 110(39): 19220-19225.
150. Bae, C. H., Nam, A. H., Park, S. M. Formation of silver nanoparticles by laser ablation of a silver target in NaCl solution. (2002) *Appl Surf Sci* 628-634: 197-198.
151. Taton, T. A., Lu, G., Mirkin, C. A. Two-color labeling of oligonucleotide arrays via size-selective scattering of nanoparticle probes. (2001) *J Am Chem Soc* 123(21): 5164-5165.
152. Cao, Y. W., Jin, R., Mirkin, C.A. DNA-modified core-shell Ag/Au nanoparticles. (2001) *J Am Chem Soc* 123(32): 7961-7962.
153. Mock, J. J., Barbic, M., Smith, D. R., et al. Shape effects in plasmon resonance of individual colloidal silver nanoparticles. (2002) *Journal of Chemical Physics* 116: 6755-6759.
154. Yang, B., Kamiya, S., Shimizu, Y., et al. Glycolipid nanotube hollow cylinders as substrates: Fabrication of one-dimensional metallic-organic nanocomposites and metal nanowires. (2004) *Chem Mater* 16(14): 2826-2831.
155. Lytton-Jean, A. K., Mirkin, C. A. A Thermodynamic Investigation into the Binding Properties of DNA Functionalized Gold Nanoparticle Probes and Molecular Fluorophore Probes. (2005) *J Am Chem Soc* 127(37): 12754-12755.
156. Hutter, E., Fendler, J.H. Exploitation of Localized Surface Plasmon Resonance. (2004) *Adv Mater* 16(19): 1685-1706.
157. Tokareva, I., Hutter, E. Hybridization of oligonucleotide-modified silver and gold nanoparticles in aqueous dispersions and on gold films. (2004) *J Am Chem Soc* 126(48): 15784-15789.
158. Roy, D., Fendler, J.H. Reflection and absorption techniques for optical characterization of chemically assembled nanomaterials. (2004) *Adv Mater* 16(6): 479-508.
159. Chiang, C. Y., Mello, C. M., Gu, J., et al. Weaving genetically engineered functionality into mechanically robust virus fibers. (2007) *Adv Mater* 19(6): 826-832.
160. Kim, J.S., Kuk, E., Yu, K.N., et al. Antimicrobial effects of silver nanoparticles. (2007) *Nanomedicine* 3(1): 95- 101.
161. Sun, R. W., Rong, C., Chung, N. P. Y., et al. Silver nanoparticles fabricated in Hepes buffer exhibit cytoprotective activities toward HIV-1 infected cells. (2005) *Chem Commun* 5059- 5061.
162. Lu, L., Sun, R.W., Chen, R., et al. Silver nanoparticles inhibit hepatitis B virus replication. (2008) *Antivir Ther* 13(2): 253- 262.
163. Sun, L., Singh, A. K., Vig, K., et al. Silver Nanoparticles Inhibit Replication of Respiratory Syncytial Virus. (2008) *J Biomed Biotechnol* 4(2): 149- 158.
164. Baram-Pinto, D., Shukla, S., Perkas, N., et al. Inhibition of herpes simplex virus type 1 infection by silver nanoparticles capped with mercaptoethanesulfonate. (2009) *Bioconjugate Chem* 20(8): 1497- 1502.
165. Rogers, J. V., Parkinson, C. V., Choi, Y. W., et al. A Preliminary Assessment of Silver Nanoparticle Inhibition of Monkeypox Virus Plaque Formation. (2008) *Nanoscale Research Letters* 3(4): 129- 133.
166. Elechiguerra, J., Burt, J. L., Morones, J. R., et al. Interaction of silver nanoparticles with HIV-1. (2005) *Nanobiotechnology* 3: 1-10.
167. Lederman, M. M., Veazey, R. S., Offord, R., et al. Prevention of vaginal SHIV transmission in rhesus macaques through inhibition of CCR5. (2004) *Science* 306(5695): 485-487.
168. Lara, H. H., Ayala-Núñez, N. V., Ixtepan-Turrent, L., et al. Mode of antiviral action of silver nanoparticles against HIV-1. (2010) *J Nanobiotechnology* 8: 1.
169. Kwong, P. D., Wyatt, R., Robinson, J., et al. Structure of an HIV gp120 envelope glycoprotein in complex with the CD4 receptor and a neutralizing human antibody. (1998) *Nature* 393(6686): 648- 659.
170. Wyatt, R., Sodroski, J. The HIV-1 envelope glycoproteins: fusogens, antigens, and immunogens. (1998) *Science* 280(5371): 1884-1888.
171. Lekutis, C., Olshevsky, U., Furman, C., et al. Contribution of disulfide bonds in the carboxyl terminus of the human immunodeficiency virus type I gp120 glycoprotein to CD4 binding. (1992) *J Acquir Immune Defic Syndr* 5(1): 78-81.
172. McDonnell, G. E. Chemical Disinfection. Antisepsis, disinfection, and sterilization. (2007) 111-115.
173. Taylor, P. L., Ussher, A. L., Burrell, R.E. Impact of heat on nanocrystalline silver dressings: Part I: Chemical and biological properties. (2005) *Biomaterials* 26(35): 7221-7229.
174. Starodub, M.E., Trevors, J.T. Silver resistance in *Escherichia coli* R1. (1989) *J Med Microbiol* 29(2): 101- 110.
175. Bhol, K.C., Schechter, P.J. Topical nanocrystalline silver cream suppresses inflammatory cytokines and induces apoptosis of inflammatory cells in a murine model of allergic contact dermatitis. (2005) *Br J Dermatol* 152(6): 1235- 1242.
176. Lawn, S.D., Butera, S.T., Folks, T.M. Contribution of immune activation to the pathogenesis and transmission of human immunodeficiency virus type 1 infection. (2001) *Clin Microbiol Rev* 14(4): 753-777.
177. Stone, A. Microbicides: a new approach to preventing HIV and other sexually transmitted infections. (2002) *Nat Rev Drug Discov* 1(12): 977-985.
178. Shattock, R.J., Moore, J.P. Inhibiting sexual transmission of HIV-1 infection. (2003) *Nat Rev Microbiol* 1(1): 25- 34.
179. Weber, J., Nunn, A., O'Connor, T. et al. 'Chemical condoms' for the prevention of HIV infection: evaluation of novel agents against SHIV(89.6PD) in vitro and in vivo. (2001) *AIDS* 15(12): 1563- 1568.
180. Bowman, M.C., Ballard, T.E., Ackerson, C.J., et al. Inhibition of HIV fusion with multivalent gold nanoparticles. (2008) *J Am Chem Soc* 130(22): 6896- 6897.
181. du Toit, L.C., Pillay, V., Choonara, Y.E. Nano-microbicides: Challenges in drug delivery, patient ethics and intellectual property in the war against HIV/AIDS. (2010) *Adv Drug Deliv Rev* 62(4-5): 532- 546.